

Photonic Entanglement for Fundamental Tests and Quantum Communication

Wolfgang Tittel

*Group of Applied Physics, University of Geneva (GAP)
20, Rue de l'Ecole-de-Médecine, 1211 Geneve 4, Switzerland*

Gregor Weihs

*Institut of Experimental Physics, University of Vienna (UNIVIE)
Boltzmannngasse 5, 1090 Wien, Austria*

Received (October 22, 2018)

Revised (October 22, 2018)

Entanglement is at the heart of fundamental tests of quantum mechanics like tests of Bell-inequalities and, as discovered lately, of quantum computation and communication. Their technological advance made entangled photons play an outstanding role in entanglement physics. We give a generalized concept of qubit entanglement and review the state of the art of photonic experiments.

Keywords: entanglement, non-locality, quantum communication

Contents

1	Introduction	3
2	The superposition principle: photonic qubits and entanglement	5
2.1	The qubit	5
2.1.1	A theoretical approach	5
2.1.2	Preparing and measuring a qubit	6
2.2	Two-particle entanglement	8
2.2.1	Photon pair sources	10
2.2.2	Types of entanglement	11
2.2.3	Measuring entanglement	15
2.3	N-particle entanglement	18
3	Fundamental tests of nonlocality	19
3.1	Bell inequalities	19
3.1.1	Closing loopholes	21
3.1.2	Relativistic configurations	25
3.2	GHZ states and nonlocality	27
4	Quantum communication	33
4.1	Quantum cryptography	33
4.1.1	Quantum cryptography based on faint laser pulses	33
4.1.2	Quantum cryptography based on photon-pairs	37
4.2	Quantum dense coding	41
4.3	Quantum teleportation	43
4.4	Entanglement swapping	44
4.5	Purification and distillation	46
5	Conclusion	50

1 Introduction

Due to its importance for understanding the properties of the quantum world and its role in applications in the new domain of quantum computation and communication, entanglement got more and more attention within the physics community throughout the last 70 years, and, lately, even in the general public.^aThe interest in entanglement, a term invented by Erwin Schrödinger in 1935¹,^bwas triggered by a paper by Einstein, Podolsky and Rosen (EPR) that was published also in 1935.² In this famous paper, often referred to as EPR paradox, the authors analyze the predictions for a two-particle state where neither particle can be considered in a state independent from the other. In contrast, both subsystems, even if at arbitrarily large distance, form a single entangled system. Based on the assumption of locality, i.e. that the choice of the type of measurement performed on one particle can not influence the properties of the other particle, they argued that the description of reality as given by the wavefunction is not complete.

The question whether or not this is true, or, in other words, whether or not entanglement (and hence non-locality) exists became a very important fundamental issue. It was Bell's discovery of the so-called Bell inequalities in 1964³ and their extension to experimental conditions by Clauser *et al.* in 1969 and 1974^{4,5} that transferred the former purely philosophical debate to the realms of laboratory experiments. Beginning with the first test of Bell inequalities in 1972,⁶ an increasing number of more and more refined experiments has been performed.^{7,8} Although the type of particles entangled is of no importance to demonstrate the existence of non-locality, by far most experiments relied on entangled photons. Nowadays, although not all experimental loopholes have been closed simultaneously in a single experiment (but all of them have already been closed), it is commonly believed that quantum non-locality is indeed real. Nevertheless, there is still interest in performing more Bell-type tests. A first motivation is to examine the boundary between the quantum and the classical world,^{9,10} a second one are experiments extending the traditional set-up for Bell-type tests to relativistic configurations and investigating so-called relativistic non-locality.¹¹ While massive particles — prone to decoherence — are used for experiments of the first kind,¹² it was again photons that served for experiments of the second kind.¹³

Apart from these fundamental motivations, the recent discovery that processing and exchange of information based on quantum systems enable new forms of computation and communication, more powerful than its classical analogs, engendered further interest in entangled systems (see i.e. Refs. [14,15,16]). Best known applications in the domain of quantum communication — hence in the domain where photons are most likely best suited for — are quantum cryptography (for a recent review see Ref. [17]) and quantum teleportation.¹⁸

In this article, we review experiments based on *photonic entanglement*, addressing both fundamental as well as applied aspects. However, although there has been considerable progress in experiments based on continuous quantum variables as well (see e.g.

^asearching the internet for “entanglement”, we found 45.000 pages!

^bEntanglement is translated from the original German word “Verschränkung”.

Refs. [19,20,21]), we will focus only on entanglement between discrete two-level quantum systems (now called quantum bits or qubits). This enables us to pursue a rather formal approach, summarizing all experiments under the aspect of experiments with entangled qubits.

The article is structured along the following lines: In Section 2 we introduce the “quantum toolbox” in form of sources and analyzers for qubits and entangled qubits, respectively, and we explain various experimental approaches. The fact that all different realizations of a qubit are formally equivalent (a qubit is a qubit) then renders the task of presenting the variety of experiments quite simple: With different arrangements of these few basic building blocks various issues can be addressed experimentally. This concerns tests of non-locality (Section 3) as well as applications of entanglement in the domain of quantum communication (section 4). As we will see, it is sometimes enough to change only minor things like analyzer settings in order to “continuously” pass from one to the other side — like from tests of Bell inequalities to quantum tomography and quantum cryptography. Finally, a short conclusion is given in Section 5.

2 The superposition principle: photonic qubits and entanglement

One of the most important features of quantum theory is certainly the superposition principle. While we find this property already in classical wave theories, e.g. in Young's famous double-slit experiment in classical optics, quantum theory allows for instance to describe objects that have traditionally been considered well localized in space as being in a superposition of different positions, well separated in space. The superposition-principle can be applied to any physical property, and it is at the origin of the "quantum-paradoxes" as well as of quantum information theory.

2.1 The qubit

2.1.1 A theoretical approach

The most important entity of classical information theory is the bit. A bit can *either* have the value "0" or "1" with both values separated by a large energy gap so that the unwanted spontaneous transition from one to the other value is extremely unlikely.^c

The quantum mechanical analog of the bit is the quantum bit or qubit. It is a two-state quantum system with the basic states $|0\rangle$ and $|1\rangle$ forming an orthogonal basis in the qubit space. In contrast to the classical bit, it is possible to create qubits in a coherent *superposition* of $|0\rangle$ and $|1\rangle$, the general state being

$$|\psi\rangle_{\text{qubit}} = \alpha |0\rangle + \beta e^{i\phi} |1\rangle \quad (\alpha^2 + \beta^2 = 1). \quad (1)$$

Qubits can be represented graphically on the qubit-sphere^d pictured in Fig. 1. The states $|0\rangle$ and $|1\rangle$ are localized on the poles of the sphere, any superposition of $|0\rangle$ and $|1\rangle$ with equal coefficients α and β are represented on the equator, and qubits with different coefficients lie on a circle with polar angle $\tan(\varphi) = \beta/\alpha$. Note that any two states represented on opposite sides of the sphere form a orthonormal basis in the two-dimensional Hilbert space describing the qubit.

In contrast to classical bits, the outcome of a measurement of a qubit is not always deterministic. For the general qubit state given in Eq. 1, one finds the value "0" with probability α^2 and the value "1" with probability β^2 . Note that this could still be achieved with a classical bit in a mixture between "0" and "1". However, the unique feature of a quantum bit is that the basic states $|0\rangle$ and $|1\rangle$ are superposed coherently. Let us consider the state

$$|\psi'\rangle = \frac{1}{\sqrt{2}} [|0\rangle + |1\rangle]. \quad (2)$$

Measuring this state in a rotated basis with eigenvectors $|0'\rangle = |0\rangle + |1\rangle$ and $|1'\rangle = |0\rangle - |1\rangle$, we always find the result "0". This contrasts with an incoherent mixture between $|0\rangle$ and $|1\rangle$ that stays a mixture in any basis and leads to either result with equal probabilities.

^cThe bit error rate in standard telecommunication is $10^{-9} - 10^{-12}$.

^dDepending on the physical property represented also known as Bloch- or Poincaré-sphere.

The transition from a coherent superposition to an incoherent one can be caused by decoherence. In contrast to the first case that is represented on the shell of the qubit sphere, an incoherent superposition can be found closer to the origin of the sphere with a completely incoherent one represented in the origin.

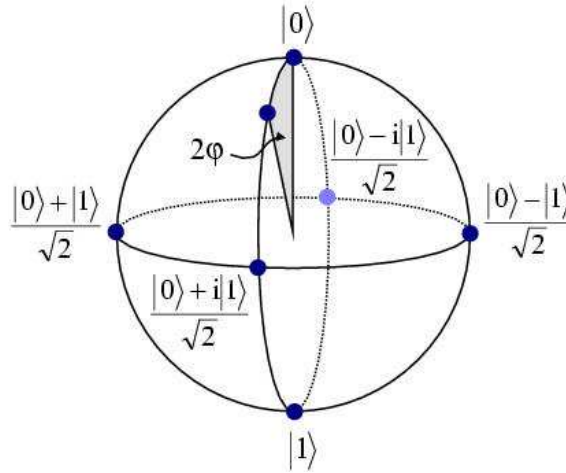


Fig. 1. The general qubit sphere. Coherent superpositions of $|0\rangle$ and $|1\rangle$ lie on the shell of the sphere, incoherent ones closer to the origin. All states represented on opposite sides on the shell of the sphere form an orthonormal basis in the two-dimensional qubit space.

2.1.2 Preparing and measuring a qubit

Although, from a theoretical point of view, a qubit is just a qubit independent of its implementation, one must identify the abstract qubit space with a physical property when planning an experiment. There are various ways in which qubits can be realized using single photons.^e Every degree of freedom that is available can in principle be exploited. The available properties are the photons' polarization, spatial mode, emission time, or their frequency.

In addition, depending on the specific goal, there are initial considerations concerning the wavelength of the photons used: If the goal is to demonstrate the existence of a certain quantum effect, it is a good idea to work at a wavelength where high efficiency and low noise single photon detectors (based on silicon avalanche photo diodes (APD)) are commercially available, hence at around 700–800 nm. If the wavelength has to be compatible with optical fibers as often requested for quantum cryptography or other long distance applications of

^eNote that the generation of a *single* photon is far from being obvious. In quantum cryptography, single photons are often mimicked by faint laser pulses with a mean photon number of 0.1.

quantum communication, the absorption of the fibers require to work in the second or third telecommunication window (at 1310 and 1550 nm, respectively). Here, only home made detectors based on Germanium or InGaAs APDs are available. Obviously, the same reflections hold for the creation of entangled qubits (Section 2.2.1) as well. For a more detailed discussion of technological issues, see Gisin *et al.*¹⁷

Polarization qubits The most well known realization of a qubit is probably the one using orthogonal states of polarization. In this case, the qubit-sphere is identical with the well-known Poincaré sphere. We identify left $|l\rangle$ and right $|r\rangle$ circular polarized photons as our basis states $|0\rangle$ and $|1\rangle$; they are represented on the poles of the sphere. Linear polarization of any orientation as an equally weighted coherent superposition of $|l\rangle$ and $|r\rangle$ can be found on the equator, and elliptically polarized light elsewhere. Completely depolarized light as an incoherent superposition of right and left circular polarized photons is represented by a point located at the origin. Polarization qubits can be created and measured using polarizers and waveplates oriented at various angles.

Spatial-mode qubits Another possibility to realize a qubit is shown in Fig. 2. Using a variable coupler and a phase shifter, Alice can create any desired superposition of a photon being in mode $|0\rangle$ and in mode $|1\rangle$. A similar set-up serves to analyze the qubit. If Bob uses for instance a symmetrical coupler and a phase $\varphi=0$, a click in detector 0 collapses the photon state to $|\psi_0\rangle = \frac{1}{\sqrt{2}}(|0\rangle + i|1\rangle)$ and in detector 1 to the orthogonal state $|\psi_1\rangle = \frac{1}{\sqrt{2}}(|0\rangle - i|1\rangle)$. Using a completely asymmetrical coupler, the photon state is projected onto the basis spanned by the states $|\phi_0\rangle = |0\rangle$ and $|\phi_1\rangle = |1\rangle$. Spatial-mode qubits would not be very practical for transmitting quantum information since the phase between $|0\rangle$ and $|1\rangle$ is easily randomized by different environments acting on the different modes.

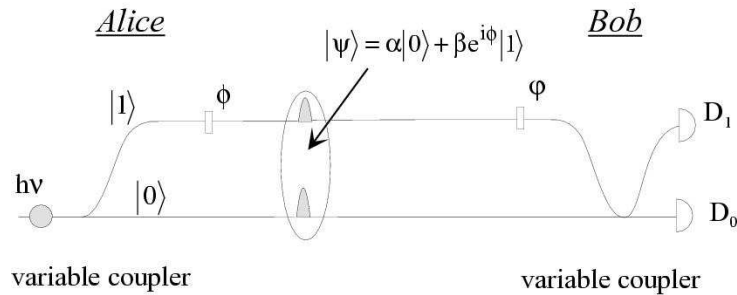


Fig. 2. Creation and measurement of a spatial-mode qubit.

Time-bin qubits A much more robust realization of $|0\rangle$ and $|1\rangle$ in so-called time-bin qubits is shown in Fig. 3. The switch at Alice's is used to transfer the amplitudes of

both spatial modes — arriving with time-difference Δt large compared to the photon’s coherence time (localization) — without losses into one mode. The net effect is to create a superposition of amplitudes describing a photon in two different time-bins. To undo this transformation, Bob uses a second switch, delaying now the amplitude of the first time-bin with respect to the amplitude of the second one so that both arrive simultaneously at the variable coupler — identically to the measurement of the mode qubit. This set-up corresponds to systems developed for faint laser-pulse based quantum cryptography (see Section 4.1) by British Telecom²², Los Alamos National Laboratory²³ and, in a modified and even more robust “plug&play” form, by one of our groups (GAP).^{24,25} The good performance of these systems underlines the robustness of time-bin qubits with respect to decoherence effects as encountered while transiting down an optical fiber.

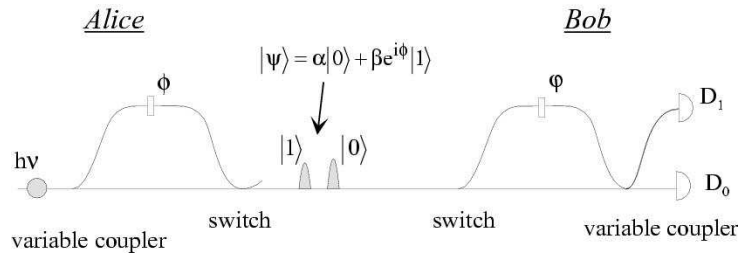


Fig. 3. Creation and measurement of a time-bin qubit.

Frequency qubits Finally, qubits can in principle be realized using a superposition of basic states at frequencies $|\omega_1\rangle$ and $|\omega_2\rangle$. This resembles much schemes in atomic physics where different energy levels are used to realize a qubit. However, the superposition of the two basic states is probably difficult to achieve with photons, and to our knowledge, no experiment has been reported to date. Note nevertheless that there is related work concerning cryptography with frequency states²⁶ or based on phase-modulated light²⁷.

Superposition in higher dimensions: qu-nits All we said so far was based on superposition of two orthogonal states. Although this is general for polarization, two dimensions are only one possibility for superpositions of different modes, emission times, frequencies, or orbital angular momenta²⁸ which are not restricted to two dimensional Hilbert space. Fig. 4 shows the straight-forward generalization of a time-bin qubit to a 4-dimensional qu-quart.²⁹

2.2 Two-particle entanglement

Entanglement can be seen as a generalization of the superposition principle to multi-particle systems, a principle which is already at the heart of the qubit. Entangled qubits can be described by

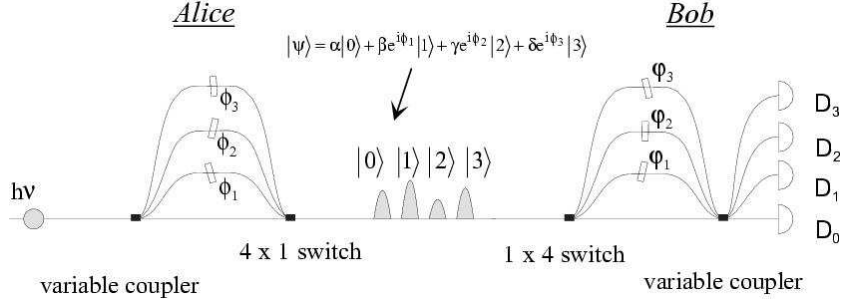


Fig. 4. Generation and detection of qu-quarts. Depending on the coupling ratios and the phases ϕ_1 to ϕ_3 , Alice can create any four dimensional time-bin state. The analyzing device at Bob's is identical to Alice's preparation device. A click in one of his detectors corresponds to the projection on one of the four eigenstates.

$$|\psi\rangle = \alpha |0\rangle_A |0\rangle_B + \beta e^{i\phi} |1\rangle_A |1\rangle_B \quad (3)$$

or

$$|\psi\rangle = \alpha |0\rangle_A |1\rangle_B + \beta e^{i\phi} |1\rangle_A |0\rangle_B \quad (4)$$

and again $\alpha^2 + \beta^2 = 1$. The indices label the entangled photons. For equal amplitudes α and β , and $\phi = 0, \pi$, Eqs. 3 and 4 reduce to the well-known Bell states

$$|\psi^\pm\rangle = \frac{1}{\sqrt{2}} (|0\rangle_A |0\rangle_B \pm |1\rangle_A |1\rangle_B) \quad (5)$$

and

$$|\phi^\pm\rangle = \frac{1}{\sqrt{2}} (|0\rangle_A |1\rangle_B \pm |1\rangle_A |0\rangle_B) \quad (6)$$

Entangled states are states where each of the entangled particles has no property of its own but where the property of the global state is well defined. This becomes clear when we look at the density matrix representations for the global and the reduced (one particle) state. Here we give the example of the ψ^- -Bell state:

$$\rho_{\text{global}} = |\psi^-\rangle \langle \psi^-| = \begin{pmatrix} |00\rangle & |01\rangle & |10\rangle & |11\rangle \\ \hline 0 & 0 & 0 & 0 \\ 0 & \frac{1}{2} & -\frac{1}{2} & 0 \\ 0 & -\frac{1}{2} & \frac{1}{2} & 0 \\ \hline 0 & 0 & 0 & 0 \end{pmatrix} \quad (7)$$

and

$$\rho_{\text{reduced}} = \text{Tr}_A(\rho) = \text{Tr}_B(\rho) = \mathbf{1} \quad (8)$$

All properties that can be used to realize photonic qubits can be used to create entangled qubits as well. Before focusing on the various realizations, we will briefly present

the two main types of photon pair sources — sources that always create photons in pairs, however, not necessarily in an entangled state.

2.2.1 Photon pair sources

Atomic cascades The first sources for entangled photons were constructed using two-photon transitions in various elements with either very short-lived or even virtual intermediate states.^{6,30,31} The most notable elements used were Ca and Hg. All these sources suffered from the common drawback that the atomic decay with two emitted photons is a three-body process. Therefore, the relative direction of one emitted photon with respect to the other is completely uncertain. This reduces the achievable collection efficiency to an extremely low value leading to numerous experimental problems.

Parametric down-conversion When Burnham and Weinberg³² discovered the production of photon pairs by spontaneous parametric down-conversion (SPDC) in 1970, they did not foresee the enormous wealth and precision of experiments that this technique would allow. Ou and Mandel^{33,34} then triggered the extensive work on entanglement from SPDC.

Spontaneous parametric down-conversion is part of a $\chi^{(2)}$ nonlinear optical effect also known as three-wave mixing. In the spontaneous case only one of the three interacting fields — usually called pump — is initially excited. The two others are in the vacuum state at first. Classically they would remain unexcited but quantum mechanically there exists a small chance that a pump photon decays into two photons which emerge within their coherence-time, ≈ 100 fs, simultaneously from the crystal.³⁵

The rate of this process scales linearly with the pump intensity and the magnitude of the nonlinear coefficient. Non-vanishing $\chi^{(2)}$ -nonlinearities can only appear in non-centrosymmetric materials. KDP (KD_2PO_4), LiIO_3 , KNbO_3 , LiNbO_3 , and BBO ($\beta\text{-BaB}_2\text{O}_4$) are a few of the most widely used crystals.

Naturally, the process of SPDC is subject to conservation of energy and momentum. The latter one is also called phase matching condition. They determine the properties of the created photons, namely their polarization, the wavelength and the direction of propagation (the mode). Phase matching can be achieved in birefringent crystals if either both, or one of the down-converted photons are polarized orthogonally with respect to the pump photons. The first type is referred to as type I phase matching, the second type as type II phase matching. If the birefringence of the crystal can not be exploited, it is possible to achieve so-called quasi phase matching in crystals where the sign of the $\chi^{(2)}$ non-linear coefficient is periodically reversed. SPDC is a very inefficient process; it needs around 10^{10} pump photons to create one photon-pair in a given mode. Lately, two groups demonstrated down-conversion in periodically poled lithium niobate waveguides,^{36,37} reporting unprecedented efficiencies as high as 10^{-6} — four orders of magnitude more than what has been achieved with bulk crystals.³⁶

Spontaneous parametric down-conversion is possible using a continuous as well as a pulsed pump (for problems associated to very short pump pulses, see Ref. [38] and references therein). The latter is necessary if the creation time of a photon pair must be determined exactly (see Sections 3.2, 4.3 and 4.4).

2.2.2 Types of entanglement

In order to produce photon pairs in entangled states (here entangled qubits), there must be two possible ways of creating such a pair — for example both photons in state $|0\rangle$ or both photons in state $|1\rangle$. First sources were based on the already mentioned cascaded transitions in atoms (Section 2.2.1), going from a well defined state of total angular momentum of the atom to another such state of lower energy. The final state could be reached via two possible ways producing polarization entangled photon pairs in its net effect. In the following, we will omit these first realizations and focus only on recent sources of entangled photons based on spontaneous parametric down-conversion. However, as already mentioned, we will neither comment on squeezed states entanglement^{19,20} nor on entanglement of external angular momentum states.²⁸ Finally, problems arising from the fact that the number of photon-pairs is (almost) thermally distributed will be addressed only in Section 4.1 (quantum cryptography). Here we assume photon-pairs in a $n=1$ Fock-state.

Polarization entanglement Most experiments to date have taken advantage of polarization entanglement. The first down-conversion sources only generated pairs of photons in product states and the entanglement was created using some additional optics. The set-ups were rather simple, but they suffered from necessary postselection by coincidence measurements. Nowadays more sophisticated configurations for down-conversion can produce polarization entanglement directly.

- Entanglement with post-selection

The first sources were so-called type-I sources, which means that the two down-converted photons carry identical polarization. Momentum conservation rules the emission directions such that two photons out of an individual down-conversion process emerge on cones centered around the pump beam. At the degenerate wavelength (twice the pump wavelength) both photons will always be on the same cone opposite of each other with respect to the pump beam.

The type-I down-conversion source can be used to produce polarization entanglement if the polarization of one of the beams is rotated by 90° before it is superposed with the other beam on a beam-splitter³⁴ (see Fig. 5). Post-selecting the cases where the photons exit in different spatial modes by means of a coincidence measurement yields polarization entanglement. An appropriate description of the post-selected state is given by

$$|\psi\rangle = \frac{1}{\sqrt{2}} [|0\rangle_A |1\rangle_B + e^{i\phi} |1\rangle_A |0\rangle_B] \quad (9)$$

where $|0\rangle$ and $|1\rangle$ stand for horizontal and vertical polarized photons. This state can easily be transformed into one of the Bell states (Eqs. 5 and 6).

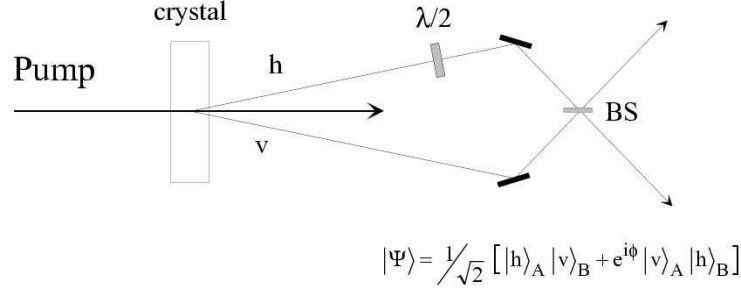


Fig. 5. Schematic of a non-collinear type-I SPDC source creating polarization entanglement after coincidence post-selection behind a beam-splitter (BS).

A more direct way to achieve polarization entanglement is type-II down-conversion where the down-converted photons are polarized orthogonally with respect to each other. In the simplest way the crystal is cut such that all beams are collinear. The pump is then separated by prisms or filters and the down-converted photons forming a pair are probabilistically separated on a beam-splitter.³⁹ Similar to the type-I source, this procedure again necessitates post-selection by coincidence techniques.

- Entanglement without post-selection

The non-collinear extension of type-II down-conversion helps to get rid of post-selection since the two down-converted photons are emitted into different spatial modes already from the beginning on. A schematic is shown in Fig. 6. This kind of source has been realized for the first time by Kwiat *et al.* in 1995.⁴⁰ The high degree of entanglement and brightness (up to 400.000 coincidence counts per second as counted with Silicon APDs) of this source made quantum teleportation and other more complicated quantum communication protocols feasible (see Section 4).

The quest for better sources and stimulated by the success of polarization entanglement from type-II sources led Kwiat *et al.*⁴¹ to invent a new scheme in which they stack two thin type-I crystals with their optic axes at 90° of each other (Fig. 7). A pump photon that has linear polarization at 45° with respect to the two optic axes will equally likely down-convert in either crystal. The photons created in the first crystal will be polarized orthogonally to the ones created in the second crystal. If the crystals are thin enough this leads to polarization entanglement. Furthermore, by varying the pump polarization one can also realize non-maximally entangled states.

Momentum or mode entanglement Rarity and Tapster have first realized momentum entanglement in 1990.⁴² A schematic is shown in Figure 8, left-hand picture.

From the emission of a non-linear crystal, two pairs of spatial (momentum, direction) modes are extracted by pinholes. Due to the phase matching conditions, photon pairs are created such that whenever a photon at frequency $\frac{1}{2}\omega_{\text{pump}} + \delta\omega$ is emitted into one of

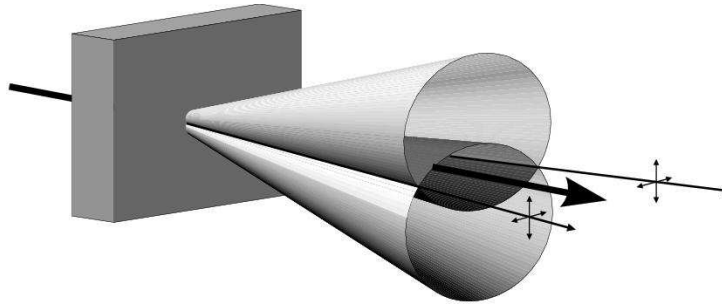


Fig. 6. Schematic of non-collinear type-II parametric down-conversion. Extraordinary (vertical, V) photons of a certain wavelength emerge on the upper cone, ordinary (horizontal, H) on the lower cone. The intersections are unpolarized and display polarization entanglement after proper compensation of the birefringent delay incurred in the conversion crystal.

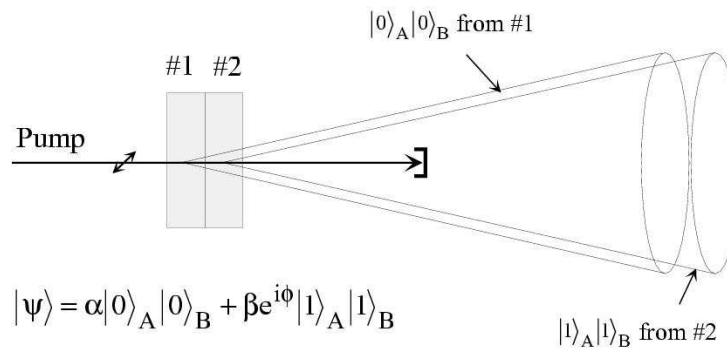


Fig. 7. Polarization entanglement using two stacked type-I down-conversion crystals with optic axis oriented at 90° with respect to each other. Depending on the polarization of the pump, maximally as well as non-maximally entangled states can be created.

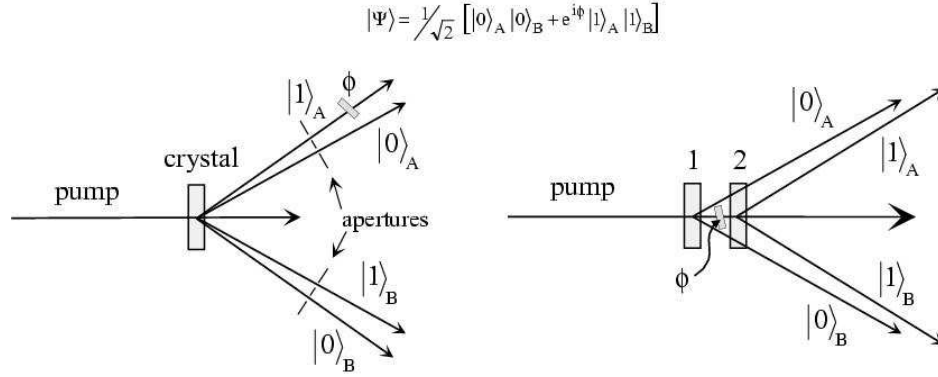


Fig. 8. Schematics of two different mode-entangled source. The phase shifter can act either locally on one of the modes as shown in the left-hand picture (Rarity *et al.*⁴²), or on both modes $|1\rangle_A$ and $|1\rangle_B$ as shown in the right-hand picture (Ribeiro *et al.*⁴³).

the inner two modes its partner at frequency $\frac{1}{2}\omega_{\text{pump}} - \delta\omega$ will be found in the opposite outer mode. The momentum entanglement very much resembles the original EPR idea of a state of two particles whose momenta are correlated in continuous space.²

Another realization has recently been published by Ribeiro *et al.*⁴³ (see right-hand side of Fig. 8). Two subsequent crystals are pumped by a laser having a coherence length larger than the distance between the crystals. The superposition of the two amplitudes describing a photon pair created either in crystal 1 or in crystal 2 leads to a mode- or momentum-entangled state.

Time-bin entanglement Using a set-up similar to the one shown in Fig. 3, Brendel *et al.*⁴⁴ proposed and realized the first source for time-bin entangled qubits in 2000 (see Fig. 9).^f A classical light-pulse is split into two subsequent pulses by means of an interferometer with a large path-length difference. Pumping a nonlinear crystal, a photon pair is created either by pulse 1 (in time-bin 1) or by pulse 2 (in time-bin 2). Depending on the coupling ratios of the couplers in the interferometer and the phase ϕ , any maximally as well as non-maximally entangled (pure) state can be realized — similar to the polarization entangled source mentioned above. Furthermore, this set-up can easily be extended to create time-bin entangled qu-nits (see also Section 5).

Energy-Time entanglement Energy-time entanglement can be considered the “continuous” version of time-bin entanglement, hence does not belong to the class of entangled qubits. It has been proposed already in 1989 (long before time-bin entanglement) by Franson⁴⁷ in connection with a novel test of Bell inequalities (see Section 3.1). Initially, Franson considered a three-level atomic system with a relatively long lifetime for the initial state ψ_1 and for the ground state ψ_3 , and a much shorter lifetime for the intermediate

^fFor related work, see also Refs. [45,46].

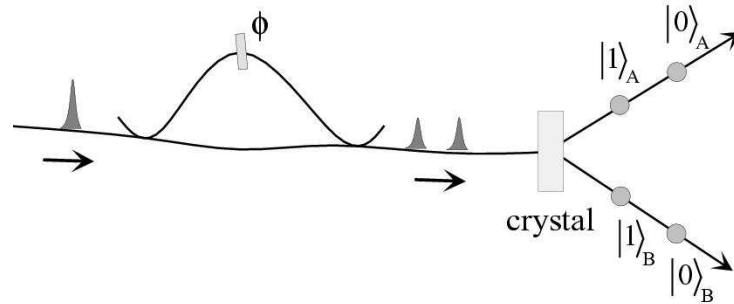


Fig. 9. Schematics of a source creating time-bin entangled qubits. Here we show a fiber-optical realization of the interferometer.

state ψ_2 (see Fig. 10). Therefore, the sum energy of both photons is very well defined although the energy of each of the two emitted photons is very uncertain. Or, in the time domain, although the precise emission time of a pair can be predicted only to within the long lifetime of the initial atomic state, both photons are emitted almost simultaneously — only depending on the short lifetime of the intermediate state.

The first to realize and employ energy-time entanglement in terms of Franson-type tests of Bell inequalities were Brendel *et al.*⁴⁸ in 1992 and, almost simultaneously, Kwiat *et al.*⁴⁹ In contrast to the initial proposal which is based on cascaded atomic transitions, both took advantage of SPDC in a non-linear crystal pumped by a coherent laser. The long coherence time of the pump-laser now bounds the emission time of a photon pair — equivalent to the lifetime of the atomic state ψ_1 — and the coherence time of the down-converted photons, which can be as small as 100 fs, determines the degree of simultaneity of the emission of the photons.

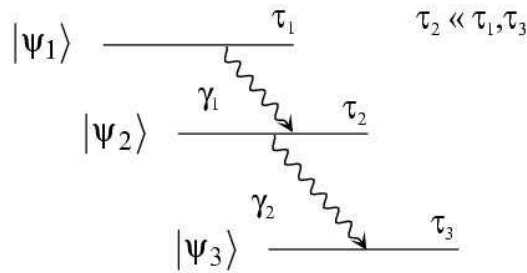


Fig. 10. Schematics for the creation of energy-time entangled photon pairs based on electronic transitions in a three-level atom. The lifetimes τ_1 and τ_3 of the initial and the final state are supposed to be large compared to the lifetime τ_2 of the intermediate state.

2.2.3 Measuring entanglement

Projection on Bell states Common to many protocols of quantum communication is the necessity to determine the state of a two particle system. For qubits, this means to project on a basis in 4-dimensional Hilbert space, spanned for instance by the four Bell states (Eq. 5 and 6). Such a measurement is known as a Bell-, or Bell-state measurement.

Figure 11 shows a possible set-up for such a measurement in the cases of polarization (left hand figure) and time-bin (right hand figure) qubits: The two particles enter a beam-splitter (BS) from modes a and b . Behind the beamsplitter, each particle is subjected to a *single qubit* projection measurement. In case of polarization qubits, this is often a projection on the horizontal and vertical axis using a polarizing beam-splitter (PBS),^{50,51} in case of time-bin qubits, the simplest way is to chose a projection on time-bins by looking at the detection time.⁴⁴ If now both photons exit the BS via different output modes (c and d , respectively) and are found to be projected on different eigenstates of the analyzers — one horizontal, one vertical, or both with one time-bin difference, respectively, — and there is no possibility to know which photon entered the BS from which mode, then the *two-photon* state is projected on the ψ^- -state. If both photons exit the BS in the same mode but are still detected in orthogonal states, then the *two-photon* state is projected on to the ψ^+ state.

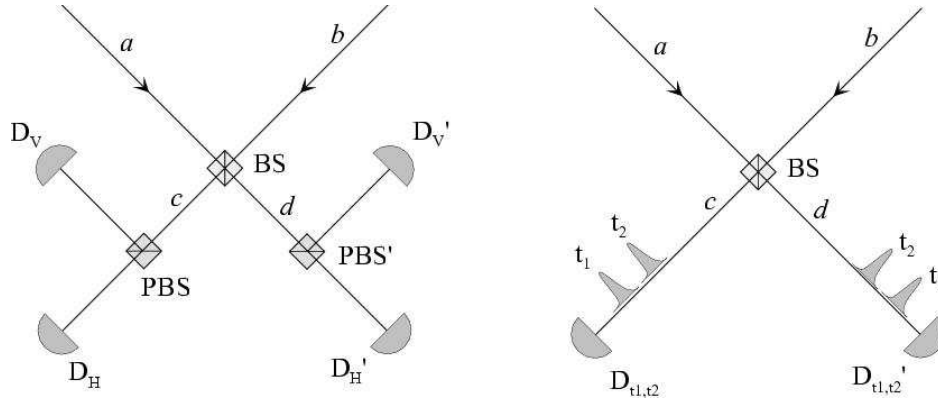


Fig. 11. Set-up using linear optics for projecting two polarization (right-hand picture) and two time-bin (left-hand picture) qubits on a basis spanned by the four Bell states. The two photons enter a beam-splitter (BS) via modes a and b and are then subjected to a polarization-, or arrival-time measurement, respectively. For polarization qubits, a coincidence between detectors D_V and D'_H (or D_H and D'_V) corresponds to a projection on the ψ^- state, a coincidence between D_V and D_H (or D'_H and D'_V) on ψ^+ . For time-bin qubits, detection of both photons in different time bins yields a projection on a ψ state: if they are found in different spatial modes on ψ^- , if they leave the beam-splitter in same spatial mode on the ψ^+ state — similar to the polarization case. Note that in both schemes only two of the four Bell states can be distinguished.

Surprisingly, as shown by Lütkenhaus *et al.*,^{52,53} there is no experimental possibility to differentiate between all of the states, at least as far as linear optics is concerned. The best one can do is to identify two of the four Bell states with the other two states leading to the same, third, result. However, as theoretically shown by Kwiat and Weinfurter in

1998, complete Bell-state analysis is possible even with linear optics if the two particles are entangled in another degree of freedom as well.⁵⁴ However, this condition can not be fulfilled by photons that come from independent sources as required e.g. for entanglement swapping (Section 4.4).

Recently, Kim *et al.*⁵⁵ performed an experiment within the frame of quantum teleportation (see Section 4.3) which could lead the way to a complete Bell measurement. The authors were taking advantage of non-linear interactions, however, even though they used a classical input, the efficiency was extremely small. Whereas in principle it would be possible to extend this method to a single photon input, which could carry any qubit realization, it does not seem feasible with current technology.

A major problem for every Bell state measurement is to erase the “identity” of the originally incoherent wave-functions. It must not be possible to infer by any degree of freedom whether a detected photon originates from a specific mode. One condition that emerges from this criterion is that the coincidence window should be significantly smaller than the coherence time of the photons (“ultracoincident”). It turns out that this situation is rather tricky to achieve in an experiment, especially if both photons come from different sources. As can be seen in Ref. [56], it involves an elaborate application of a quantum erasure technique using mode-locked pulsed lasers to make the coincidence window independent of any electronic limitations while still maintaining reasonable count rates.

Quantum state reconstruction The most general approach to measure a quantum state is the reconstruction of its density matrix (also called quantum tomography). In the case of two-qubit states, this has first been investigated by White *et al.* in 1999⁵⁷ for polarization qubits. Obviously, this method can be generalized to any realization of a qubit. The measuring scheme is depicted in Fig. 12. In contrast to the Bell-state measurements mentioned before, not only one projection has to be measured, but the density matrix is reconstructed from the statistical outcomes of different joint projection measurements.

In general there is some freedom in the choice of the measurements that will ultimately be performed. A density matrix for a partially mixed state in a d -dimensional Hilbert space contains $d^2 - 1$ independent parameters. Therefore one needs at least as many independent measurements to be able to reconstruct such a matrix. For a two-qubit state this would be 15 measurements.

Still, in general it is difficult to calculate the matrix elements given only some marginal probabilities. Of course, it is possible to just directly invert the set of measurement results but taking into account the ubiquitous measurement errors it turns out that direct inversion is not always suitable because it can sometimes even lead to unphysical density matrices.⁵⁸ A different approach — this was also applied to experimental data in Ref. [59] — is the maximum likelihood method, in which a suitably chosen likelihood functional is maximized by the physical state that is most likely to having produced the given measurement results.

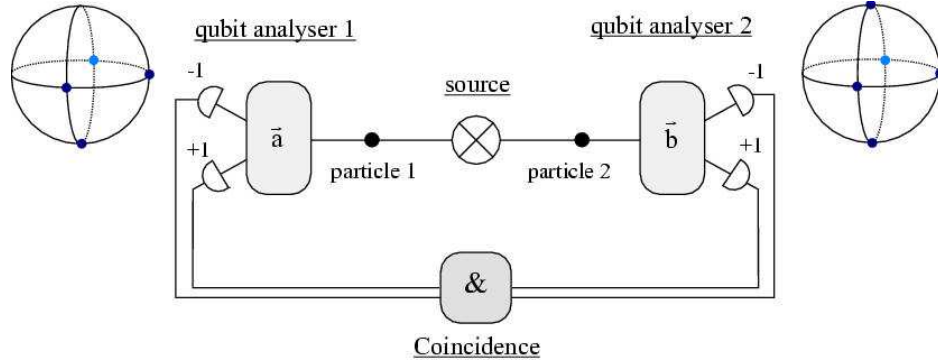


Fig. 12. Schematics for reconstruction of the density matrix of a two-qubit state. Each of the two particles is analyzed using a qubit-analyser. The vectors \vec{a} and \vec{b} specify the bases to be projected on. Note that the eigenvalues of the different bases lie on a two-dimensional subspace within the shell of the respective qubit-spheres.

2.3 N-particle entanglement

With the pioneering work by Greenberger *et al.*⁶⁰ it became clear that entangled states of three or more particles are very important for fundamental tests of quantum theory. Also, applications in quantum communication like quantum secret sharing have been found that require multi-particle entanglement.^{61,62}

Although the interest in GHZ states is quite high, no efficient practically usable sources have been discovered to date.⁹ As long as deterministic quantum gates are not available we depend on combining two-particle entangled states and projective measurements to construct entangled states of three or more particles by postselection.^h Examples of this technique will be presented in Section 3.2.

Just as in the two particle case these higher entanglements could in principle be prepared for any degree of freedom (for time-bin entanglement see Ref. [44]), and methods for GHZ state analysis have been suggested.⁶⁵ Still, as long as there is no efficient way to produce these states, the corresponding applications will probably remain in the academic interest only. An exception is the quantum secret sharing scheme explained in Section 4.1.2, where GHZ state correlations are mimicked by the correlations observed between the pump photon and the two downconverted photons.⁶⁶

⁹One might speculate about a generalization of parametric down-conversion to processes, where more than two photons are generated. However, the corresponding non-linear coefficients are generally many orders of magnitude lower than in the parametric down-conversion case. As we restricted ourselves to photonic entanglement, it would be beyond the scope of this article to discuss many-particle entanglements that have been produced with Rydberg atoms and ions in a trap.^{63,64}

^hAs always, postselection means that a state is not actually prepared at any stage in the experiment. Still, it is possible to observe the correlations that quantum theory predicts for the specific state.

3 Fundamental tests of nonlocality

3.1 Bell inequalities

Since the early days of quantum physics the intrinsic randomness of measurement outcomes puzzled many physicists. Even very prominent proponents believed that there should be a more complete, “realistic” theory complementing quantum physics with some “extra” information in order to be able to describe the observed randomness in classical terms of statistical ensembles. This “extra” information has become widely known as “hidden variables”.^{67,68} A state of a system with a certain set of hidden values would then be called dispersion-free or super-pure.

The debate whether or not hidden variable theories correctly describe nature was triggered in 1935 by the now famous paper by Einstein, Podolsky and Rosen (EPR).² However, the debate remained a purely philosophical one until 1964, when Bell derived a statement which is in principle experimentally testable.^{3,69} He started from EPR’s example in the version given 1957 by Bohm.⁷⁰ The latter considered a gedankenexperiment where a source emits pairs of spin-1/2 particles — we would now call them qubits — into opposite directions (see Fig. 13). The particles are analyzed by two independent “qubit-analyzers”: Stern-Gerlach apparatus in separate regions of space. From the idea of spatial separation, the assumption of locality, namely that the setting of the analyzer on one side can not influence the properties of the particle on the other side, is inferred as a very natural restriction for any otherwise most general hidden-variable model. Bell found that the correlation between the two measurements as predicted by any such model must necessarily comply with a set of inequalities nowadays known as Bell inequalities. The most widely used form reads

$$S(\mathbf{a}, \mathbf{b}, \mathbf{a}', \mathbf{b}') := |\mathbf{E}(\mathbf{a}, \mathbf{b}) - \mathbf{E}(\mathbf{a}, \mathbf{b}')| + |\mathbf{E}(\mathbf{a}', \mathbf{b}') + \mathbf{E}(\mathbf{a}', \mathbf{b})| \leq 2, \quad (10)$$

where $E(\mathbf{a}, \mathbf{b})$ is the correlation coefficient of measurements along \mathbf{a}, \mathbf{a}' and \mathbf{b}, \mathbf{b}' . S is sometimes called Bell-parameter and has the meaning of a second-order correlation.

It is easily seen that a singlet state of two spin-1/2 particles (the ψ^- Bell state) will violate this inequality with $S = 2\sqrt{2}$ for a specific set of analyzer directions. We conclude that a system governed by local hidden variables (LHV) — a system that can be described by a local theory — cannot mimic the behaviour of entangled states and hence that quantum theory must be a non-local theory. It is interesting to note that the set-up for testing Bell inequalities is identical to the one needed to measure the density matrix of a two-qubit state as explained in Section 2.2.3. Only, in order to get the full information about a quantum system, there are more analyzer directions to measure than when testing whether the two-particle system is correctly described by a local or by a non-local theory.ⁱ

ⁱ Another approach to see whether hidden variable theories can mimic the quantum behaviour is based on the concept of non-contextuality. This means that the measured value of an observable should not depend on the context, i. e. other commuting observables, that are measured simultaneously. Kochen and Specker⁷¹ and independently Bell⁷² showed that given an at least three dimensional Hilbert space and

Shortly after Bell's discovery it became clear that no existing experimental data could be used to find out whether or not non-local behaviour can indeed be observed. Furthermore it turned out that there were still some problems in applying the inequality to real experiments because of shortcomings of sources, analyzers, and detectors. These shortcomings are usually called loopholes (see Section 3.1.1) because they leave an escape route open for local realistic theories. To arrive at a logically correct argument against LHV one has to supplement the "strong" original Bell inequalities with additional assumptions which allow to calculate the necessary correlation coefficients from the measured coincidence count rates (see paragraph 3.1.1). Such modified "weak" inequalities as derived e.g. 1969 by Clauser, Horne, Shimony and Holt (CHSH)⁴ (Eq. 10), or 1974 by Clauser and Horne,⁵ were then used in most experiments to interpret the data.

By today all these shortcomings have been eliminated, though not all of them simultaneously in one experiment. The overwhelming evidence suggests that indeed quantum physics accurately describes nature and that LHV theories have been ruled out.

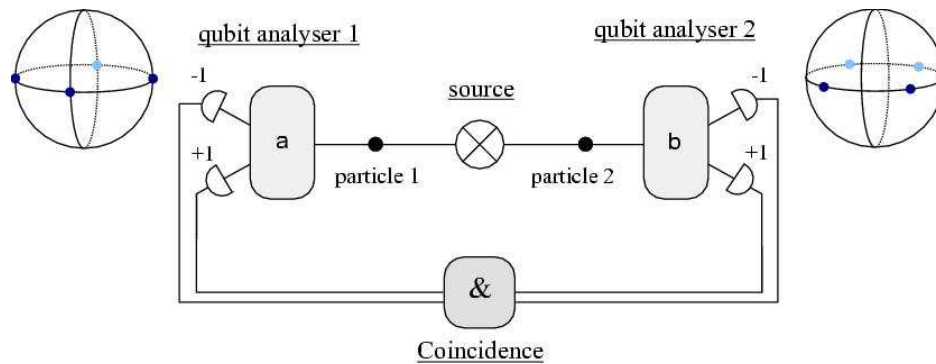


Fig. 13. General set-up for Bell experiments. A source emits correlated particles, each of which can be described in a two-dimensional Hilbert space. The qubits then fly back to back towards two qubit analyzers making projection measurements in bases defined by parameters a and b , respectively. The outcomes of the measurements are correlated, enabling to test via Bell inequalities whether the two-particle system can be described by a local or by a non-local theory. Note that it is sufficient to project on two different bases with eigenvalues located on a one-dimensional subspace within the shell of the respective qubit-spheres, in contrast to quantum tomography (Section 2.2.3).

In the following we will present a brief history of Bell experiments, give an account of the current state-of-the-art and discuss the experiments that were instrumental in closing the loopholes.

starting from the assumption of non-contextuality, it is indeed possible to prove a theorem against hidden variables. For many years it was an open question how to experimentally test the Bell-Kochen-Specker theorem. Last year, Simon *et al.*⁷³ proposed an experiment based on measurements on a single particle that is in an entangled state of two different degrees of freedom.

History The following table is a necessarily incomplete account of events in the history of tests of Bell inequalities. More experiments can be found in Refs. [74,30,31,75,39,76,40,77,78,79,80].

- 1972 Freedman and Clauser perform the first experimental test based on polarization entangled photons generated via cascaded atomic transitions, demonstrating that indeed a Bell inequality is violated for an entangled system and thus ruling out a local realistic description.⁶
- 1982 Aspect *et al.* measure polarization correlations with two-channel analyzers.⁸¹ Later they carry out an experiment in which they vary the analyzers during the flight of the particles under test.⁸²
- 1988 Ou and Mandel and independently Shih and Alley do the first non-locality experiments using parametric down-conversion sources to create polarization entanglement.^{34,83}
- 1990 Rarity and Tapster observe momentum entanglement in their experiment.⁸⁴
- 1992 Brendel *et al.*⁴⁸ and a bit later Kwiat *et al.*⁴⁹ realize Franson's idea of a test based on energy-time entanglement.⁴⁷ Although the source itself does not produce entangled qubits directly (see Section 2.2.2), the use of qubit-analyzers post-projects on such states.
- 1997 Tittel *et al.* show that the quantum correlations between energy-time entangled photons are preserved even over distances of more than 10 km.^{85,86}
- 1998 Weihs *et al.* close the spacelike separation (Einstein locality) loophole using randomly switched analyzers. This experiment was based on polarization entanglement.⁸⁷
- 2001 Rowe *et al.* perform the first test violating a strong Bell inequality. In contrast to all other tests that were based on photons, this experiment took advantage of entangled ions.⁸⁸

Current status As can be seen from this table, various types of entanglement have been used for tests of Bell inequalities. In addition, Tittel *et al.* recently employed time-bin entangled photons for quantum cryptography (see Section 4.1), an experiment that can be interpreted as a test of Bell inequalities as well.⁸⁹ This supports the notion of a completely abstract formulation of Bell's gedankenexperiment in terms of two apparatus each with a variable parameter that produce output correlated results. The generalization of the original formulation based on Bohm's example of two spin 1/2 particles and Stern Gerlach apparatus can for instance be found in a paper by Mermin.⁹⁰

Presently parametric down-conversion sources (s. Section 2.2.1) in various configurations deliver the highest quality entangled states. The entanglement contrast can be as high as 99.5% while maintaining reasonable count rates. In terms of standard deviations and coincidence count rates, some of the most impressive violations of Bell inequalities were published in Refs. [40,91].

3.1.1 Closing loopholes

As already stated above, there are certain loopholes in most of the realized experiments. Here we discuss their current status from the experimentalist's perspective

Detector efficiency Pearle⁹² first noticed already in 1970 that in real tests of Bell's inequality, which fall short of detecting all particles that are emitted by the source, one can still construct a hidden variable model that accurately predicts the observed data (see also recent work by Santos⁹³ and by Gisin⁹⁴). Afterwards this argument has been named efficiency loophole because of the fact that various inefficiencies reduce the ratio of counted to emitted particles sometimes to less than a few percent. These inefficiencies include incomplete collection of particles from the source, imperfect transmission of optical elements and analyzer devices, and most important, the far-from ideal detectors.

Violation of a Bell inequality without any supplementary assumption requires an overall efficiency of more than 82.8%. For photon based experiments this is very difficult to achieve with present photon counting technology. The threshold can be reduced to 67% by the help of non-maximally entangled states.⁹⁵ In both cases the experimental visibility must be perfect. Although in principle there exist detectors which have high enough efficiency, it is practically very unlikely that a photonic Bell experiment could achieve these efficiency levels. To date, all these experiments invoked so-called "fair sampling"⁴ and "no-enhancement" assumptions⁵ which allow to derive inequalities into which only coincidence count rates enter. However, very recently a beautiful experiment based on two entangled ions in a microscopic trap succeeded in violating a strong Bell inequality at nearly 100% efficiency.⁸⁸ Many physicists consider this a closure of the discussed loophole.⁸

Separation Spatial separation is an important ingredient in the derivation of Bell's inequality. The lack of large spatial separation does not by itself constitute a loophole but it was said that with increasing distance the quantum correlations could diminish.⁹⁶ Therefore it is natural to try to extend the range of proven quantum phenomena to as large a distance as possible. In addition, the fact that, and the question how entanglement can be maintained over large distances is very important for quantum communication protocols like quantum cryptography (see also Section 4.5).

The largest spatial separation has been achieved in tests that were carried out by one of our groups (GAP) in 1997 and 1998.^{85,86,97} The experiments utilized energy-time entanglement created by parametric down-conversion at a wavelength of 1310 nm, suitable for transmission in standard telecommunication optical fibers. Clear violations of Bell inequalities of up to 16 standard deviation were achieved for measurements that were more than 10 km apart (see Figs. 14 and 15).

Einstein locality The other prominent loophole in experiments on Bell's inequality is called the "spacelike separation" or "Einstein locality" loophole.⁹⁸ It is constituted by the fact that for most experiments it was possible to explain the observed correlations by a hypothetic subluminal (slower than or equal to the vacuum speed of light) link between the two particles or apparatus and particles. Given such a link it would in principle be

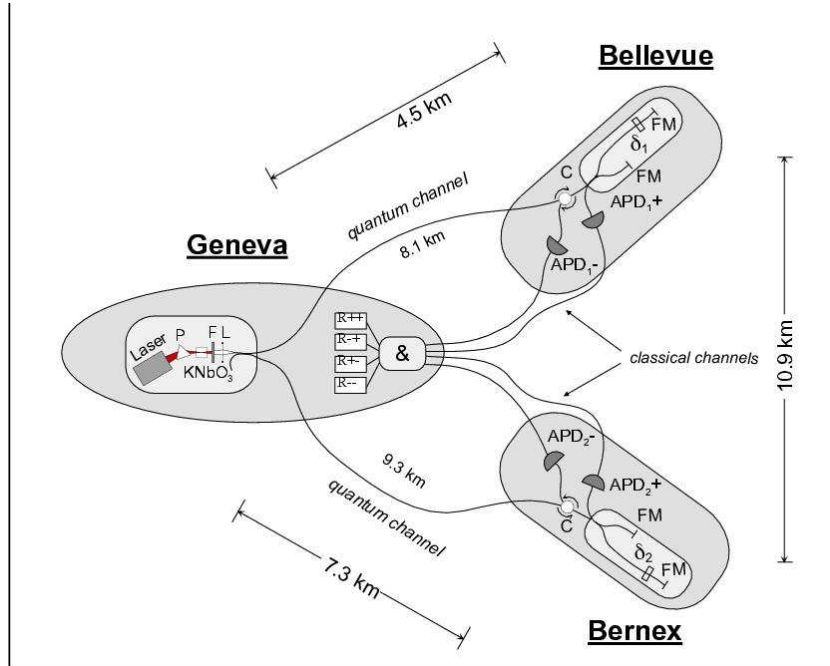


Fig. 14. Experimental arrangement for a test of Bell's inequality with measurements made more than 10 km apart. Source (in Geneva) and observer stations (interferometers in Bellevue and Bernex, respectively) were connected by a fiber optic telecommunications network.

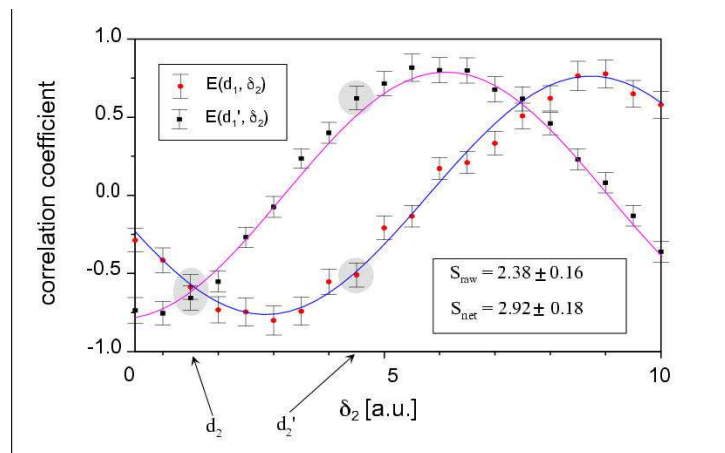


Fig. 15. Data from the long distance Bell test. The two curves show the correlation coefficients for two different analyzer settings at Alice's while varying the setting at Bob's. A clear violation of the CHSH inequality is observed.

possible that the analyzer direction or even the measurement outcome is communicated to the other side.

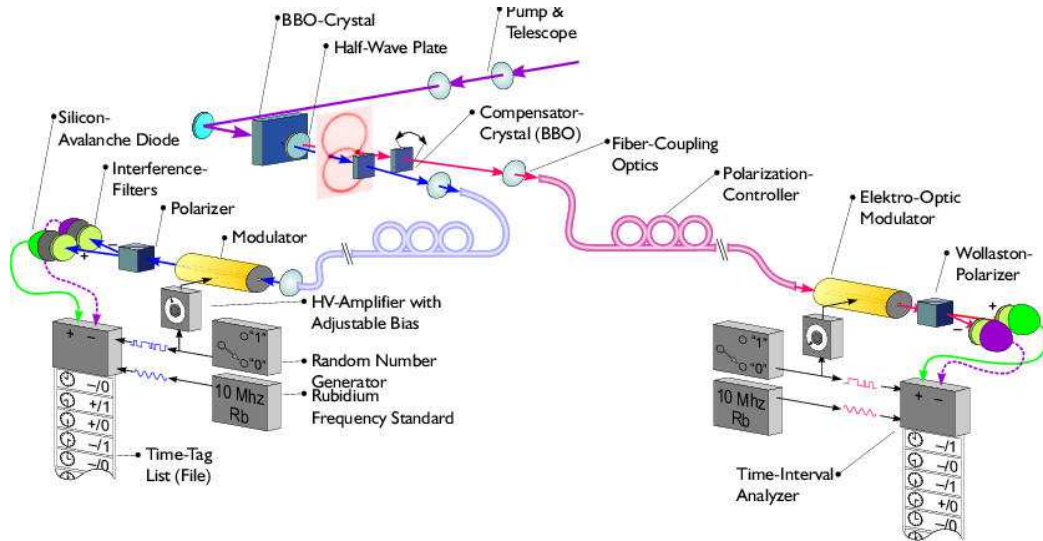


Fig. 16. Experimental set-up for a test of Bell's inequality with independent observers. Data are collected locally at the observer stations only and can be compared after the measurement is completed.

Bell himself considered this fact as being important, calling it “the vital time factor”.⁹⁹ However, operationally and theoretically it is hard to define this “time factor”. There is no criterion that is generally agreed upon. Bohm talked already in 1957 about variation of the analyzers while the particles are in flight.⁷⁰ Over the years the idea emerged that it would be necessary to vary the analyzers in a random way, where the randomness would have to be drawn from local sources or from distant stars in opposite directions of the universe. Including the generation of randomness and other delays the measurements should then be completed within a time that is short compared to the time it takes to signal to the other observer station. This prescription amounts to performing the measurement in spacelike separated regions of spacetime.

Obviously these are extremely vague concepts and therefore it is not astonishing that only two experiments have tried to pin down and answer these questions. The first one was performed by Aspect *et al.*⁸² in 1982 and included a periodic variation of the analyzers. Because periodic functions are in principle predictable it has been said that this experiment was not definitive in closing the spacelike separation loophole.

In 1998, 16 years later, one of our groups (UNIVIE) was able to include the randomness factor and, at the same time, to extend the spatial separation to 360 m yielding a large safety margin for the spacelike separation issue.⁸⁷ The experimental set-up is shown in Fig. 16. It yielded a violation of Bell's inequality by 30 standard deviations.

Another approach to attack the locality loophole has been demonstrated by Tittel *et*

al. in 1999.⁹⁷ In this experiment, two analyzers with different parameter settings were attached to each side of the source, and the random choice was done by a passive optical coupler, sending the photons to one or the other analyzer. Hence, in contrast to the experiment mentioned before, the randomness does not come from an external random number generator but is engendered using the photons themselves and might therefore seem “less good”.^j

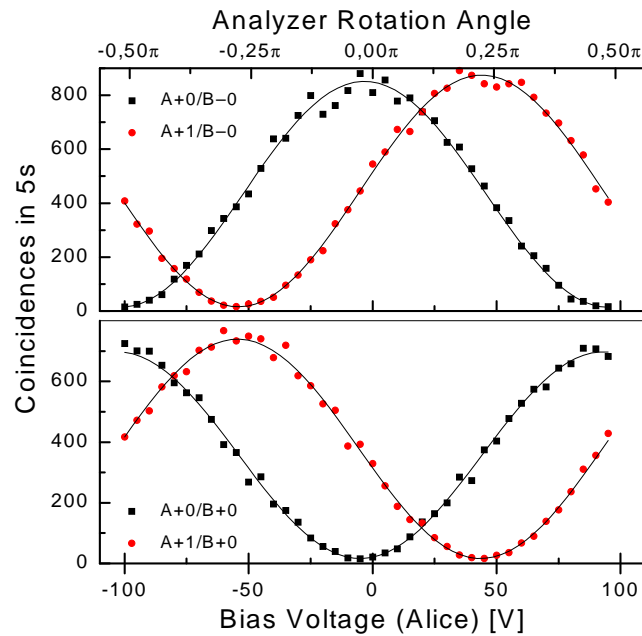


Fig. 17. Correlation curves taken for spacelike separated measurements on a polarization entangled photon pair at a distance of 360 m. The measurements yield a violation of Bell’s inequality by 30 standard deviations.

3.1.2 Relativistic configurations

To find the quantum mechanical predictions for the results of Bell-type measurements, one can think of the first measurement (traditionally at “Alice’s”) as a non-local state preparation for the photon traveling to the second analyzer (at “Bob’s”) — like in entanglement based quantum cryptography (Section 4.1.2): In a first step one calculates the probabilities for the different outcomes of Alice’s measurement that depend only on the setting of her analyzer and the *local* quantum state.^k Knowing the *global* two-particle state enables in a second step to calculate Bob’s *local* state. In a third step, equivalent to the

^jHowever, note that the borderline between “good” and “bad” randomness is very vague.¹⁰⁰

^kThe local state is obtained by tracing over the distant system. In case of a maximally entangled global state, it is completely mixed and the outcome of Alice’s measurement is completely random.

first one, one calculates the probabilities of the different outcomes of the measurement at Bob's (which are now joint probabilities), determined by his local state — hence by the setting of the first analyzer and the specific two-particle (global) state used — and by the setting of the second analyzer.

Many people believe that the state vector is not endowed with reality but that it is only a mathematical tool that helps to calculate the statistical outcomes of experiments. Consequently, the reduction of the state of Bob's subsystem by Alice's measurement must be understood as an instantaneous modification of the *knowledge* of an observer of the first measurement concerning the quantum state of the second particle. Indeed, possessing only the second system, it is impossible to see any change as a result of the first measurement: The density matrix describing the local state remains unchanged and thus there is no possibility for superluminal signaling and hence no contradiction with special relativity.¹⁰ However, it has never been proven experimentally whether the state vector does indeed not represent reality and that the collapse only changes the *knowledge* of the observer, or whether the state vector is real and its collapse has to be considered a *real physical phenomenon* as assumed e.g. by Ghirardi, Rimini and Weber.¹⁰¹

The speed of quantum information. If one assumes the collapse to be real, it is natural to ask how fast it propagates from Alice's to Bob's subsystem. The lower bound of this “speed of quantum information” (or, following Einstein's words, the speed of the “spooky action at a distance”) can easily be calculated from the distance between both analyzers (the distance that has to be traveled) and the time left for the second particle until reaching its analyzer. However, before doing so, one still has to define which parts of the analyzers are considered crucial for the alignment. The most natural choice seems to be the detectors where the transition from quantum to classical takes place, although there are other possibilities as well.^{102,11} It is assumed in the following that the important parts are indeed the detectors. From standard Bell experiments, one already knows that quantum information propagates faster than with the speed of light c . However, these experiments have not been devised in order to investigate the lower bound, and the precision of the alignment is not discussed in most works. In 2001, Zbinden *et al.*¹³ reported on an experiment performed again with analyzers separated by more than 10 km (similar to Fig. 14) where the fibers connecting the source with the detectors, this time each of 10 km length, were aligned such that the arrival time difference was smaller than 5 ps. This allowed to set a lower bound of the speed of quantum information of $2/3 \times 10^7 c$ as seen from the laboratory (Geneva) reference frame. Obviously, this is not the only possible choice of a reference frame but one can argue that this is a very natural one.

The speed of quantum information is very important for a class of problems that can be labeled “the search for a covariant description of the measurement process” with the example of the impossibility of a causal description of the instantaneous collapse in an EPR experiment that would be valid in all frames. The introduction of a preferred frame PF that would allow a realistic (obviously non-local) description of the quantum measurement is a way out of these problems.¹⁰³ However, the introduction of a PF is still an intellectual tool (or trick) and there is no experimental evidence to support this

hypothesis. A good candidate for such a preferred frame is the frame from which the cosmic microwave background radiation (CMB) is seen to be isotropic. Analyzing the same data and taking into account the relative motion between the Geneva and the CMB frame, Scarani found a lower bound of the speed of quantum information of $2 \times 10^4 c$ as seen from the CMB frame.¹⁰⁴ Repeating this experiment with different alignments, each corresponding to simultaneous measurements in a different frame, it would be possible to test whether there is one (the preferred) frame from which the speed of quantum information is seen to be limited.¹⁰⁵

Moving detectors in different reference frames. The experiment establishing the lower bound of the speed of quantum information has been extended¹³ to perform a first test of relativistic non-locality (RNL)(or multisimultaneity) — a theory unifying non-locality and relativity of simultaneity that was proposed in 1997 by Suarez and Scarani.¹¹ RNL predicts that the quantum correlation should disappear in a setting where both analyzers are in relative motion such that each one in its own inertial frame is considered to cause the collapse. In the initial proposal, the crucial part of an analyzer was assumed to be the last beamsplitter. In the experiment, it was supposed again that the alignment has to take into account the positions of the detectors. Although many assumptions concerning the nature of a detector had to be made in order to make this experiment feasible^l, it was possible for the first time to test an interpretation of quantum mechanics. The data always reproduced the quantum correlations regardless the motion of the detectors, yielding thus *experimental* evidence that the tested version of RNL does not correctly describe nature, and making it more difficult to consider the collapse of the wave function as a real phenomenon.

3.2 GHZ states and nonlocality

In 1989 (G)reenberger, (H)orne, and (Z)eilinger⁶⁰ found that entangled states of at least three quantum systems can exhibit contradictions with local realistic models that are much more striking than those found for two particles in violations of Bell inequalities: Not even the perfect correlation predicted by quantum mechanics for coincidence measurements between more than two particles can be described by realistic models. The basic set-up for such a GHZ-type test is shown in Fig. 18. While it became clear later, that, from a fundamental point of view, there is no difference between GHZ- and Bell-type tests of non-locality, at the conceptual level the so-called GHZ correlations remain a remarkable feature of quantum physics.

Naturally, people have tried to construct such states and investigate their properties but as there are no efficient and controllable natural sources for three or more photon states the researchers had to resort to techniques allowing to construct higher dimensional

^lFor example, it was assumed that a black absorbing surface is sufficient to engender the collapse of the wave function: A detected photon can *in principle* be observed, e.g. via increase of the temperature of the black surface. This is similar to the fact that it is sufficient to observe distinguishability *in principle* to make the fringes in an interference experiment disappear.

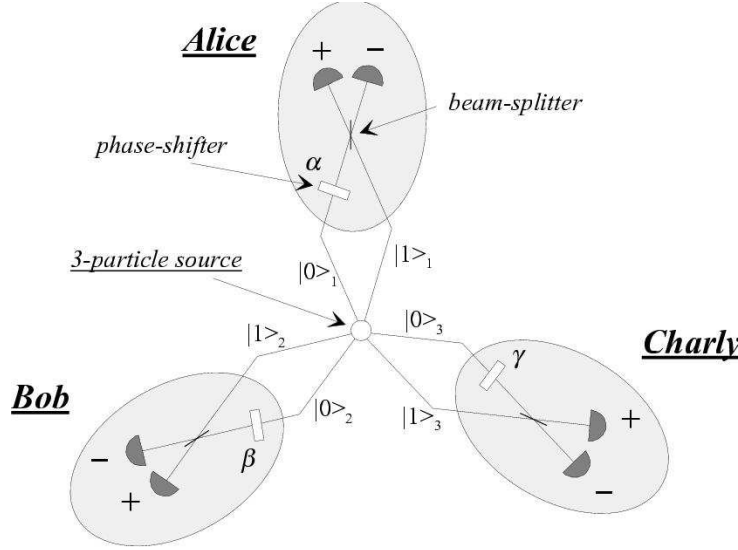


Fig. 18. Schematics for a test of 3-particle GHZ-type non-locality using momentum entangled states. The three qubits are each sent to an analyzer. Coincidence measurements in identical or orthogonal bases enable to test whether the three-particle state is described by a local, or by a non-local model. Note that, in contrast to Bell-type tests of non-locality, only settings leading to deterministic outcomes — either perfect coincidences or perfect anti-coincidences — are required.

entanglement from two-particle entangled states (see Section 2.3).

Generation of three-photon entangled states. In 1999 Bouwmeester *et al.*¹⁰⁶ reported the first observation of three-particle entanglement. The team employed two photon pairs produced in non-collinear parametric downconversion from a pulsed UV pump beam and combined them via beam-splitters to a conditional three particle-entangled state. The schematic (Fig. 19) shows that whenever a trigger photon is received and simultaneously photons are observed in modes 1–3, in subsequent correlation measurements (not shown) one will observe results which can only be described by the state

$$\frac{1}{\sqrt{2}} |H\rangle_T [|HHV\rangle_{123} + |VVH\rangle_{123}]. \quad (11)$$

The fact that such a state exists must be considered a manifestation of quantum non-locality.

While Bouwmeester demonstrated the existence of a three-photon GHZ state, Pan *et al.*¹⁰⁷ reported last year the first and still only experiment in which the test against local realism was carried out in full. Although GHZ-type tests theoretically permit a clear cut contradiction to local realism, in a real experiment one has to resort to an inequality just like in Bell's theorem. For this task, Pan measured in total 32 (4 groups of 8) different combinations of polarizer settings, and the reasoning followed Mermin's

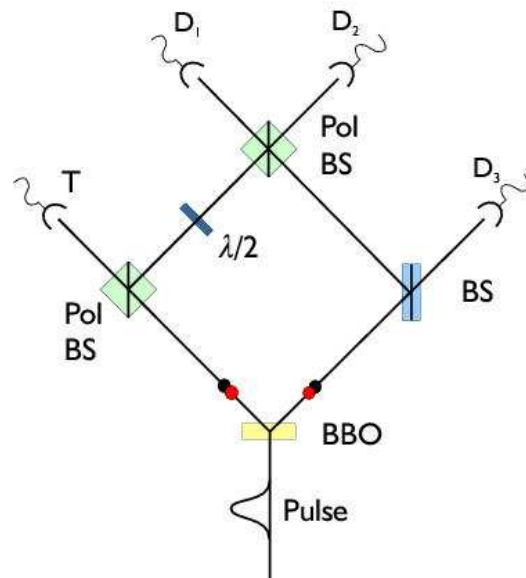


Fig. 19. Schematic of the set-up used by Bouwmeester *et al.* to produce three-photon GHZ correlations. Two independent pairs are generated simultaneously and one photon from each pair is sent “right”, one “left”. By action of the left polarizing beam-splitter (PBS), only horizontally polarized particles can reach the trigger detector T. To register three-fold coincidences between detectors 1, 2, and 3, the other photon must be reflected from that PBS, i.e. it must be vertically polarized. This photon is subsequently rotated by 45° and can end up as V in detector 1 or as H in detector 2. The only two possible ways that a triple coincidence event arises in detectors 1, 2, and 3 are therefore when the right two photons split at the right beam-splitter and when the two photons meeting at the upper PBS have identical polarization — either both horizontal or both vertical.

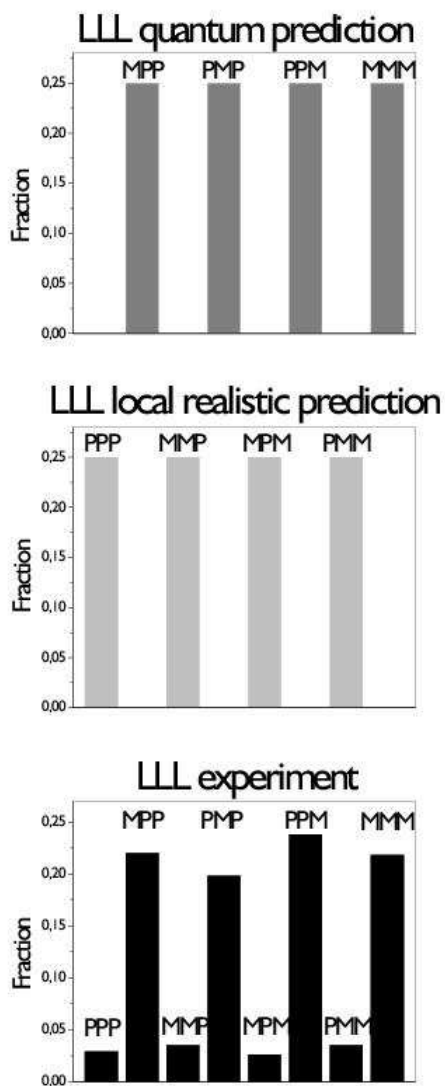


Fig. 20. The graphs show the relative frequencies of three-fold coincidence events between outputs D_1 , D_2 , and D_3 as predicted and as measured (bottom). All analyzers project onto a L =linear 45° basis. “P” and “M” refer to plus and minus 45° linear polarization, respectively. MPM for example marks the probability to measure a three-fold coincident event if polarizer settings are M for particle 1, P for particle 2, and M for particle 3. The data violate the local realistic prediction by 10 standard deviations.

argument for an entangled system of three spin-1/2 particles,¹⁰⁸ adapted to an imperfect (noisy) experimental set-up. Fig. 20 shows the results of the measurements of one of the four groups and compares them to the local realistic as well as to the quantum predictions. The data clearly violates the local realistic prediction, and agrees within experimental errors with quantum physics.

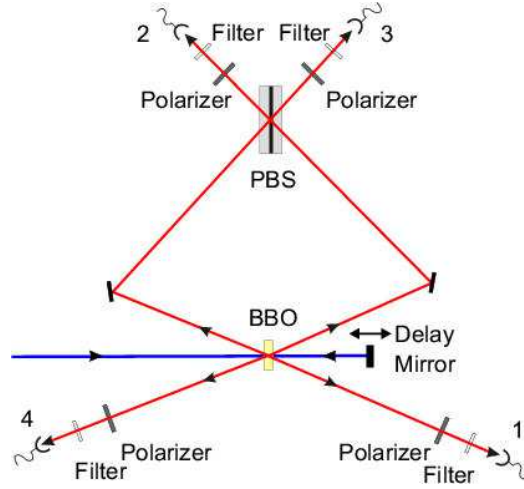


Fig. 21. Experimental set-up to create and confirm the existence of a four-photon GHZ states.

Four-photon GHZ Extending the teleportation and entanglement swapping experiments discussed in sections 4.3 and 4.4, one of our groups (UNIVIE) recently succeeded in demonstrating four-photon entanglement.¹⁰⁹ In this experiment again two down-conversion pairs are used as an initial resource, but this time from processes occurring in different spatial modes. One photon of each pair is directed towards a polarizing beam splitter. (s. Fig. 21) Coincidence detection after this beam-splitter projects the incoming product state of two entangled photon pairs onto a four-photon GHZ state.^m

$$|\Psi\rangle_{1234} = \frac{1}{\sqrt{2}} (|H\rangle_1 |V\rangle_2 |V\rangle_3 |H\rangle_4 + |V\rangle_1 |H\rangle_2 |H\rangle_3 |V\rangle_4). \quad (12)$$

A comparison of the measured 4-photon coincidence probabilities for various combinations of H and V projections confirms that indeed only the desired $|H\rangle_1 |V\rangle_2 |V\rangle_3 |H\rangle_4$ and $|V\rangle_1 |H\rangle_2 |H\rangle_3 |V\rangle_4$ components have been created. The contrast in this measurement was of more than 100:1. In addition, measurements in the conjugate 45° basis (s. Fig. 22) demonstrate the coherent superposition of the two components, hence show the existence of a four photon GHZ state and confirm the existence of non-locality.

^mNote that the state is never realized as a freely propagating system.

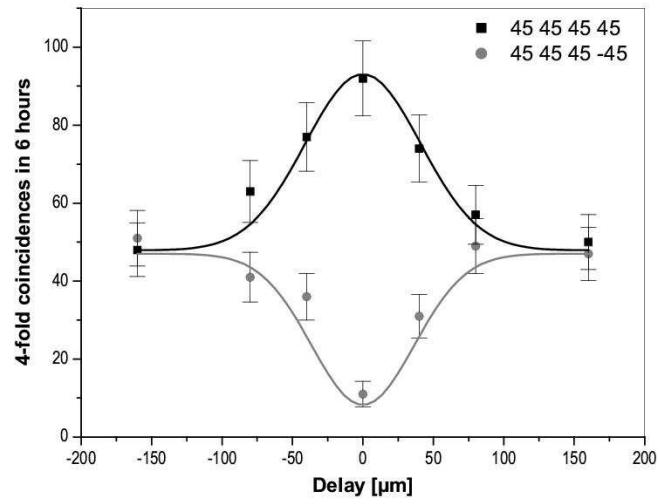


Fig. 22. Experimental data showing four-photon polarization correlation in the 45° linear basis. At zero delay between the two photons that are superposed on the polarizing beam-splitter, indistinguishability is granted and interference occurs, demonstrating the coherent superposition of $|H\rangle_1 |V\rangle_2 |V\rangle_3 |H\rangle_4$ and $|V\rangle_1 |H\rangle_2 |H\rangle_3 |V\rangle_4$.

4 Quantum communication

4.1 Quantum cryptography

Quantum cryptography (QC) is certainly the most mature application of quantum communication. Based on the non-classical feature of the quantum world, it provides two parties, a sender Alice and a receiver Bob, with a means to distribute a secret key in a way that guarantees the detection of any eavesdropping (Eve): Any information obtained by an unauthorized third party about the exchanged key goes along with an increase of the quantum bit error rate (QBER) of the transmitted data which can be checked using a suitable subset of the data. It has been shown that, as long as the QBER of the sifted key (the key after bases reconciliation) is below a certain threshold (11 or 15 %, respectively, depending on the eavesdropping strategy assumed^{110,111}), Alice and Bob can still distill a secure key by means of classical error correction and privacy amplification protocols.¹¹² This secret key can then be used together with the one-time pad to exchange a confidential message in complete privacy.

There is vast literature covering theoretical as well as experimental aspects of quantum cryptography. Since there is an extensive and very recent article¹⁷ reviewing both sides, we will keep this section short and give only the necessary information to understand *entanglement-based* quantum cryptography.

4.1.1 Quantum cryptography based on faint laser pulses

The first QC protocol has been published by Bennett and Brassard in 1984,ⁿ it is known today as BB84 or four-state protocol.¹¹⁴ Fig. 23 illustrates the protocol with the example of four polarization qubits of linear polarization. However, any property can in principle be used to realize a qubit. Furthermore, any four states that fulfill the requirement that they form two bases in the qubit space and that any two states belonging to a different basis have an overlap of $\frac{1}{2}$ will do as well.

The first experimental demonstration of quantum cryptography took place in 1989 at IBM when Bennett *et al.* realized the so-called B92 (or two-state) protocol¹¹⁵ based on polarization coding with “single photons” over a distance of 30 cm in air.¹¹² Since then, a lot of experimental progress has been made, and from 1995 on, several groups demonstrated that quantum cryptography is possible outside the laboratory over distances of tens of kilometers as well.¹⁷ All experiments relied on faint laser pulses – strongly attenuated pulses that contain less than 1 photon on average — to mimic single photons. These realizations could, even today, provide secure communication in case cryptographic protocols that are based on mathematical complexity turn out to be unsafe. However, they still suffer from low bit-rates,^o and the maximum span with today’s technology is only of around 100 km.

ⁿThe work was inspired by an unpublished article by Wiesner from 1970 (published only in 1983¹¹³)

^oTo give an example, the secret key rate (after error correction and privacy amplification) reported by Ribordy *et al.*¹¹⁶ over a distance of 23 km was of 210 Hz.

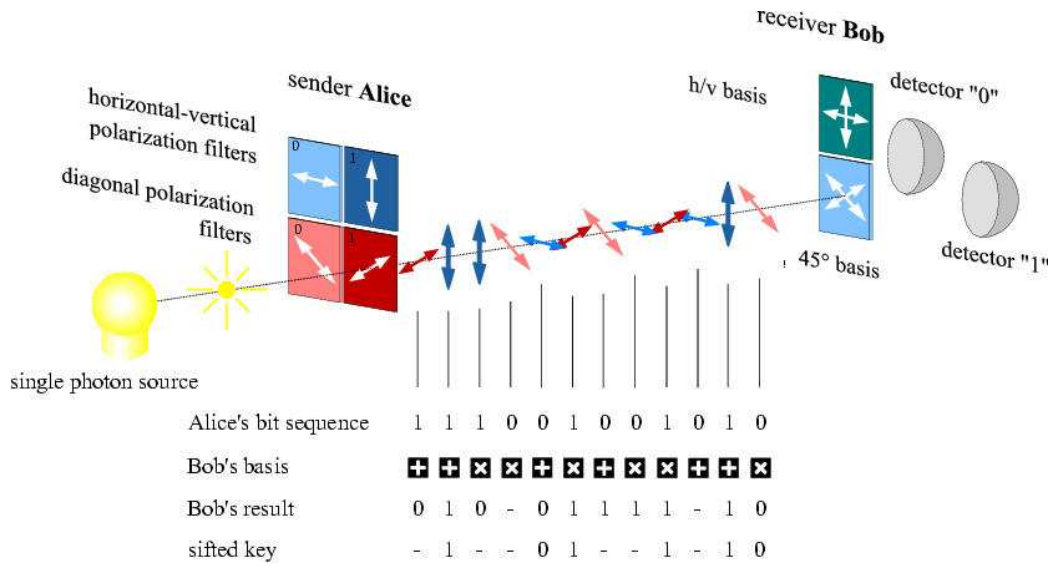


Fig. 23. For each photon she sends to Bob, Alice chooses randomly a bit value (row 1) and a basis (h/v, or $\pm 45^\circ$), and prepares the photon in the corresponding state. Every time Bob expects a photon to arrive, he activates his detectors and chooses randomly to analyze in the h/v basis, or in the $\pm 45^\circ$ basis. He records which basis he used (row 2) and, in case of a successful detection, which result (in terms of bits) he got (row 3). After exchange of a sufficient large number of photons, he publicly announces the cases where he detected a photon and the basis used for the measurements. However, he does not reveal which results he got. Alice compares event by event whether or not Bob's analyzer was compatible to her choice of bases. If they are incompatible or if Bob failed to detect the photon, the bit is discarded. For the remaining bits (row 4), Alice and Bob know for sure that they have the same value. These bits form the so-called sifted key. The security of the key distribution is, roughly speaking, based on the fact that a measurement of an unknown quantum system will, in most cases, disturb the system: If Alice's and Bob's sifted keys are perfectly correlated, no eavesdropper tried to eavesdrop the transmission and the key can be used for encoding a confidential message using the one-time pad. If the sifted keys are not 100% correlated, then, depending on the QBER, Alice and Bob can either distill a secret key via error correction and privacy amplification, or the key is discarded and a new distribution has to be started.

Let us briefly elaborate on the maximum distance. In theory, i.e. using perfect experimental equipment, the sifted key rate decreases exponentially with increasing transmission losses but never drops to zero. It is given by the product of Alice's pulse rate f_{rep} , the number of photons per pulse μ , the probability t_{link} that a photon arrives at Bob's, and the quantum efficiency η that it is detected.

$$R_{\text{sifted}} = \frac{1}{2} \cdot f_{\text{rep}} \cdot \mu \cdot t_{\text{link}} \cdot \eta \quad (13)$$

The factor $1/2$ is due to key sifting — the fact that Alice and Bob use compatible bases in only 50 % of the cases. In practice, there are always experimental imperfections, and there will always be some errors in the sifted key — even in the absence of an eavesdropper. For the sake of the presentation, we assume here that the errors are only due to detector dark counts (a signal generated by a detector without the presence of a photon), arising with probability p_{dark} :

$$R_{\text{wrong}} \approx R_{\text{dark}} = \frac{1}{2} \cdot \frac{1}{2} \cdot f_{\text{rep}} \cdot p_{\text{dark}} \cdot n \quad (14)$$

The first factor $1/2$ is again due to key sifting, the second one to the fact that a detector dark count leads only in half of the cases to a wrong result, and n is the number of detectors. Finally, the QBER is given by

$$QBER = \frac{R_{\text{wrong}}}{R_{\text{sifted}}} \approx \frac{n \cdot p_{\text{dark}}}{2 \cdot t_{\text{link}} \cdot \eta \cdot \mu} \quad (15)$$

Since Alice and Bob can never know for sure whether the observed QBER is due to the imperfections of their equipment, or whether it is engendered by the presence of an eavesdropper, they always have to assume to worst case, i.e. that there is an eavesdropper that has the maximum information compatible with the observed QBER. Therefore, they have to apply classical error correction and privacy amplification protocols to the sifted key in order to distill a secret key.

Fig. 24 shows the secret bit rate after error correction and privacy amplification as a function of distance. Here we assume that the photons are transmitted using optical fibers with losses of 0.2 dB/km. The bit rate decreases exponentially for small distances. Then, with larger distance (i.e. with decreasing transmission probability t_{link} , hence increasing QBER), the bit reduction due to error correction and privacy amplification gets more and more important, and at a QBER (hence distance) where the Alice-Bob mutual Shannon information is equal to Eve's Shannon Information, there are no bits left and the curve representing the bit rate drops vertically to zero. Note that the maximum distance does not depend on Alice's pulse rate.

To achieve a better performance of a cryptographic system concerning bit rate or maximum transmission distance, there are basically two things to improve: the detectors, and the sources.

- Today's *single photon detectors*, capable of counting photons at telecommunication wavelength of 1.3 and 1.5 μm where fiber losses are low, feature quantum efficiencies

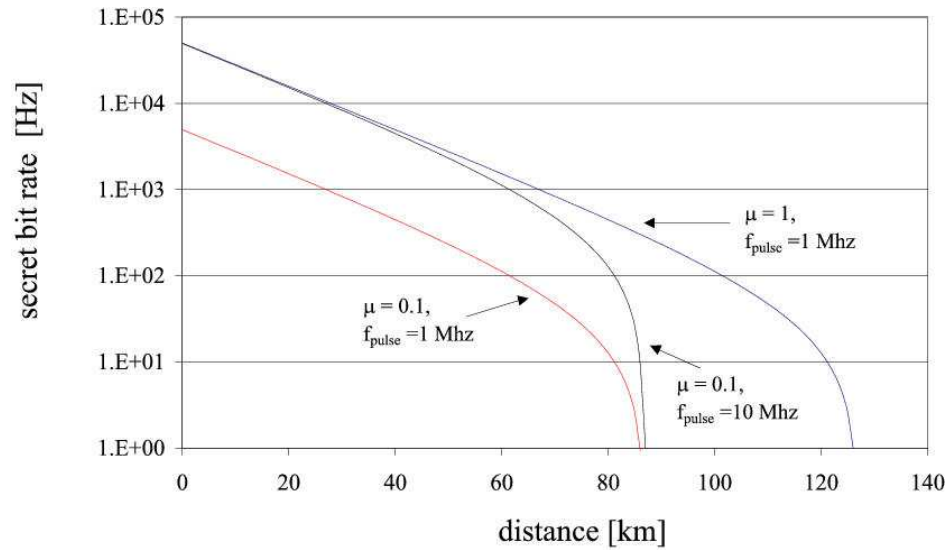


Fig. 24. Secret bit rate after error correction and privacy amplification. The maximum transmission span is given by the distance where the QBER equals 15% (assuming symmetric individual eavesdropping attacks¹¹⁰). Here we assume a initial pulse rate f_{pulse} of 1 and 10 MHz, respectively, losses of 0.2 dB/km of optical fibers at 1550 nm wavelength (close to the fundamental limit), a quantum efficiency of 10%, dark count probability of 10^{-5} and a mean photon number per pulse μ of 0.1 and 1, respectively. The use of a higher mean photon number leads to a higher secret bit rate for a given distance and pulse rate, as well as to a larger maximum transmission span, i.e. 130 instead of 90 km. A higher pulse rate engenders a higher secret key rate, however, does not change the maximum span. In practice, if we take into account non-ideal error correction and privacy amplification algorithm, multi-photon pulses and other optical losses not considered here, the maximum distance is likely to be reduced by a factor of around two.

of only around 10%, paired with a high dark count probability of $\approx 10^{-5}$ per 1 ns time window. These figures determine the secret key rate for a given distance and pulse rate, and the maximum transmission span as shown in Fig. 24. In addition, the detectors' performance limits the pulse rate via the effect of so-called afterpulses: These are avalanches that are not caused by the detection of a photon but by the release of charges from trapping levels populated while a current transits through the diode. Since the probability for observing an afterpulse after a detection of a photon decreases exponentially with time, they can be suppressed using suitable dead times — with the drawback of limiting the maximum pulse rate. It is thus obvious that the use of better detectors would have an important impact on experimental quantum cryptography.

- Mimicking single photons by *faint pulses* has a very important advantage: it is extremely simple. Unfortunately this advantage is paired with two drawbacks. First, a mean photon number smaller than 1 (the upper limit for quantum cryptography) leads to a reduction of the bit rate (see Eq. 13 and Fig. 24). Second, since the photon-number statistics for faint pulses is given by a Poissonian distribution, there is always a possibility to find more than one photon in a weak pulse. This opens the possibility of an eavesdropper attack based on multi-photon splitting.^{117,118} The smaller the mean number of photons per pulse, the smaller this threat, however, the smaller the bit rate as well.

4.1.2 Quantum cryptography based on photon-pairs

“Single-photon” based realizations In order to get around the problem of faint pulses where the probability of having zero photons in a pulse is rather high, a good idea is to replace the faint pulse source by a photon-pair source (see Section 2.2.1 and Fig. 25b) where one photon serves as a trigger to indicate the presence of the other one.¹¹⁹ In this case, Alice can remove the vacuum component of her source, and Bob's detectors are only triggered whenever she sends at least one photon.^p This leads to a higher sifted key rate (assuming the same trigger rate than in the faint-pulse case) and a lower QBER for a given distance (for given losses) and therefore to a larger maximum span (see Fig. 24). It is important to note that photon-pairs can not be created in Fock states, similar to single photons mimicked by faint pulses. Therefore, depending on the probability to create more than one photon pair, the danger of multi-photon splitting eavesdropping attacks exists as well.

Entanglement based realizations Finally, the potential of a source creating entangled pairs is not restricted to create two photons at the same time — one serving as a trigger for the other one. It is possible to use the full quantum correlation to generate identical keys at Alice's and Bobs, and to test the presence of an eavesdropper via a test of a Bell inequality (see Fig. 25c). This beautiful application of tests of Bell inequalities has been

^pHere we assume that the collection efficiency for the photon traveling towards Bob is 1. In practice, a more realistic value is ≈ 0.70 .

pointed out by A. Ekert in 1991¹²⁰ — without knowing about the “discovery” of quantum cryptography by Bennett and Brassard 7 years earlier. The set-up is similar to the one used to test Bell inequalities with the exception that Alice and Bob each have to choose from three different bases. Depending on the bases chosen for each specific photon pair, the measured data is either used to establish the sifted key, to test a Bell inequality, or it is discarded.

The security of the Ekert protocol is very intuitive to understand: If an eavesdropper gets some knowledge about the state of the photon traveling to Bob, she adds some hidden variables (hidden in the sense that only the eavesdropper knows about their value). If she gets full knowledge about all states, i.e. the whole set of photons analyzed by Bob can be described by hidden variables, a Bell inequality can not be violated any more. If Eve has only partial knowledge, the violation is less than maximal, and if no information has leaked out at all, Alice and Bob observe a maximal violation.

However, the Ekert protocol is not very efficient concerning the ratio of transmitted bits to the sifted key length. As pointed out in 1992 by Bennett *et al.*¹²¹ as well as by Ekert *et al.*,¹²² protocols originally devised for single photon schemes can also be used for entanglement based realizations. This is not surprising if one considers Alice’s action as a non-local state preparation for the photon traveling to Bob (see also Section 3.1.2). Interestingly, it turns out that, if the perturbation of the quantum channel (the QBER) is such that the Alice-Bob mutual Shannon information equals Eve’s maximum Shannon information, then the CHSH Bell inequality (Eq. 10) can not be violated any more.^{123,110} Although this seems very natural in this case and a similar connection has recently been found for n-party quantum cryptography and some n-particle Bell inequalities¹²⁴, it is not clear yet to what extent the connection between security of quantum cryptography and the violation of a Bell inequality can be generalized.

Compared to the faint pulse schemes, entanglement based QC features two advantages. First, similarly to photon-pair based realizations, Alice removes the vacuum component of her source. Actually, the entanglement based case is even more efficient since even the optical losses in Alice’s preparation device are now eliminated as can be seen from Fig. 25c.

Second, even if two pairs are created within the same detection window — hence two photons travel towards Bob within the same pulse — they do not carry the same bit, although they are prepared in states belonging to the same basis. Beyond this passive state preparation, it is even possible to achieve a passive preparation of bases using a set-up similar to the one depicted in Fig. 25d. There is no external switch that forces all photons in a pulse to be measured in the same basis but each photon independently chooses its basis and bit value. Therefore, eavesdropping attacks based on multi-photon pulses do not apply in entanglement based QC. However multi-photon pulses lead to errors at Bob’s who detects from time to time a photon that is not correlated to Alice’s.

Although all Bell experiments intrinsically contain the possibility for entanglement based QC, we list here only experiments that have been devised in order to allow a fast change of measurement bases.

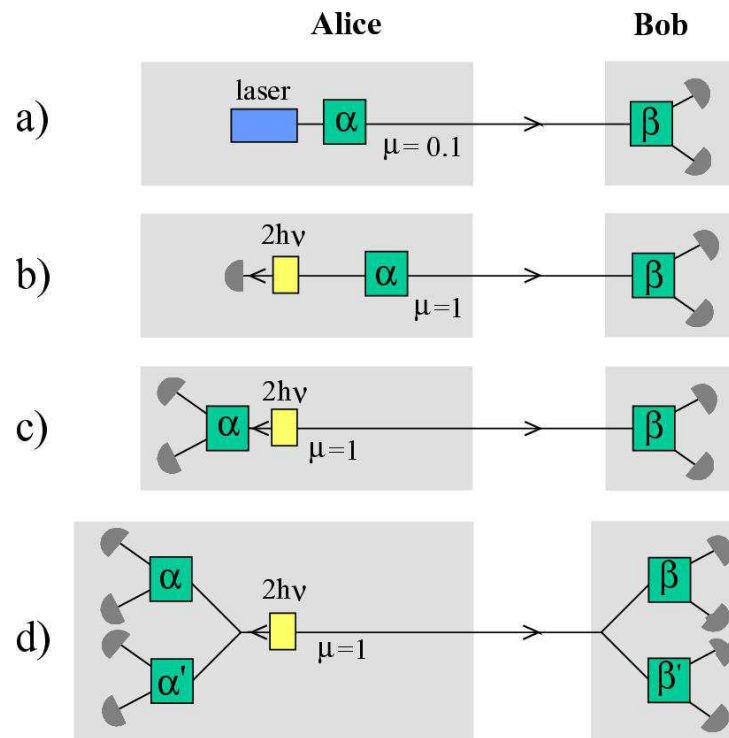


Fig. 25. Single photon based quantum cryptography using a) a faint-pulse source, b) a two-photon source, c) entanglement based quantum cryptography with active, and d) with passive choice of bases. “ $2h\nu$ ” denotes the photon-pair source, and the parameters α and β characterize the settings of the qubit-analyzers.

- 1982 Interestingly enough, the first experiment that fulfills the above definition is the test of Bell inequalities using time-varying analyzers, performed by Aspect *et al.*⁸² with polarization entangled qubits in order to close the locality loophole (see also Section 3.1.1) — at a time where quantum cryptography was not yet known, not even the single photon based version.
- 1998 Weihs *et al.* demonstrate a violation of Bell inequalities with polarization entangled qubits at 700 nm wavelength and randomly switched analyzers, separated by 360 km of optical fiber.⁸⁷ This experiment has been devised to close the locality loophole.
- 1999 Tittel *et al.* perform a Bell experiment, again to be seen in the context of the locality loophole, incorporating a passive choice of bases.⁹⁷ Two fiber-optical interferometers are attached to each side of a source creating energy-time entangled photons at 1.3 μm wavelength. However, similar to both before-mentioned experiments, the bases chosen for the measurements are chosen in order to allow a test of Bell inequalities and not to establish a secret key.
- 2000 Three publications on entanglement based cryptography appear in the same issue of Phys. Rev. Lett.:
- 1.) Using a set-up similar to the one mentioned already in the second entry of this table, Jennewein *et al.* realize a quantum cryptography system including error correction over a distance of 360 m.¹²⁵ Two different protocols are implemented, one based on Wigner's inequality (a special form of Bell inequality), the other one following BB84. Sifted key rates of around 400 and 800 bits/s, respectively, are obtained, and QBERs of around 3% observed. Using the same assumptions that lead to Fig. 24, this amounts to a secret key rate of 300 and 600 bits/s, respectively.
 - 2.) Naik *et al.* demonstrate the Ekert protocol in a free space experiment over a short (laboratory) distance.¹²⁶ The experiment takes advantage of polarization entangled qubits at a wavelength of around 800 nm. Sifted key rates of around 10 bits/s paired with a QBER of 3% are reported, leading to a secret key rate of 6 bits/s after implementation of error correction and privacy amplification. In addition to the key exchange, the authors simulate different eavesdropping strategies and find an increase of the QBER with increasing information of the eavesdropper, according to theory. The experiment has recently been extended¹²⁷ to realize the so-called six state protocol.^{128,129}
 - 3.) Tittel *et al.*⁸⁹ report on a fiber-optical realization of quantum cryptography in a laboratory experiment using the BB84 protocol. This experiment is based on time-bin entangled qubits at telecommunication wavelength of 1.3 μm and takes advantage of phase-time coding and a passive choice of bases. Sifted key rates of 33 Hz and a QBER of 4% are obtained, leading to a calculated secret key rate of 21 bits/s.
- 2001 Ribordy *et al.*¹³⁰ realize a QC system based on energy-time entanglement. In contrast to the schemes mentioned before, this realization takes advantage of an asymmetric set-up, optimized for QC, instead of a set-up designed for tests of Bell inequalities where the source is generally located roughly in the middle between Alice and Bob. Here, one photon (at 810 nm wavelength) is sent to a bulk-optical interferometer, located directly next to the source, the other one (at 1550 nm wavelength) is transmitted through 8.5 km of fiber on a spool to a fiber optical interferometer. Implementing the BB84 protocol and a passive choice of bases, a sifted key rate of 134 bits/s and a mean QBER of 8.6% (over 1 hour) is observed. From these values, one can calculate a secret key rate of 45 bits/s.

Three party quantum cryptography In addition to the mentioned two-party QC schemes, Tittel *et al.* reported in 2001 a proof-of principle demonstration of quantum secret sharing (three party quantum cryptography) in a laboratory experiment.⁶⁶ This rather new protocol enables Alice to send key material to Bob and Charlie in a way that neither Bob nor Charlie alone have any information about Alice's key, however, when comparing their data, they have full information. The goal of this protocol is to force both of them to collaborate.

In contrast to proposed implementations using three-particle GHZ states,^{61,62} pairs of time-bin entangled qubits were used to mimic the necessary quantum correlation of three entangled qubits, albeit only two photons exist at the same time (see Fig. 26). This is possible thanks to the symmetry between the preparation interferometer acting on the pump pulse and the interferometers analyzing the down-converted photons. Indeed, the data describing the emission of a bright pump pulse at Alice's is equivalent to the data characterizing the detection of a photon at Bob's and Charlie's: all specify a phase value and an output, or input port, respectively. Therefore, the emission of a pump pulse can be considered as a detection of a photon with 100% efficiency, and the scheme features a much higher coincidence count rate compared to the initially proposed GHZ-state type schemes.

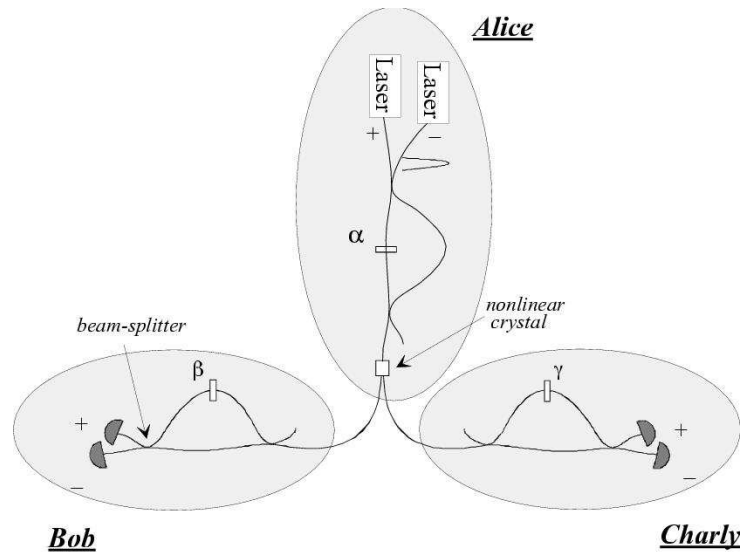


Fig. 26. Basic set-up for three-party quantum secret sharing using “pseudo-GHZ states”. Compare with “true” GHZ states as shown in Fig. 18.

4.2 Quantum dense coding

Whenever two parties A (Alice) and B (Bob) wish to communicate, they first have to

agree on a coding procedure, that is, they have to associate symbols with physical states. In classical communication, one usually uses a two letter alphabet where the different symbols (bit-values) are represented by (classical) optical pulses with different individual properties. In quantum physics we can encode information in a novel way into joint properties of elementary systems in entangled states, leading in principle to the possibility to transmit two bits of information by sending only one qubit. This striking application of quantum communication is known as quantum dense coding.

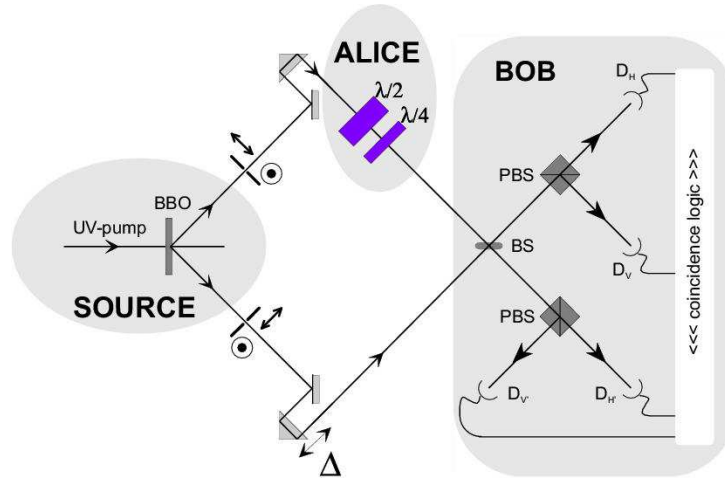


Fig. 27. Experimental set-up to demonstrate quantum dense coding based on Bell state analysis of entangled polarization qubits.⁵¹ After locally preparing the joint state of the entangled particles by means of wave-plates, Alice sends her particle to Bob. Performing a Bell measurement on the two-particle state, Bob can distinguish between two different Bell states ($|\Psi^\pm\rangle$), with the two other ones ($|\Phi^\pm\rangle$) leading to the same, third, result. Therefore, Alice can encode 1.58 bit of information sending only one qubit.

The maximally entangled Bell basis (Eqs. 5 and 6) has a very important and interesting property which was exploited by Bennett and Wiesner¹¹⁵ in their proposal for quantum dense coding: In order to switch from any one of the four Bell states to all others, it is sufficient to manipulate only one of the two qubits locally. Thus, the sender, Alice, can actually encode two bits of information into the whole entangled system by just acting on one of the two qubits.

In order to read out this information, the receiver, Bob, needs to be able to identify the four Bell states, that is, he needs to perform a Bell measurement as explained in Section 2.2.3. However, using linear optics, only two out of the four Bell states can be distinguished unambiguously^{52,53} whereas the other two states lead to identical signatures. Still, as has been experimentally demonstrated in 1996 by Mattle *et al.*,⁵¹ this is enough to encode three-valued information (corresponding to 1.58 bit of information) into each transmission event (see Fig. 27).

4.3 Quantum teleportation

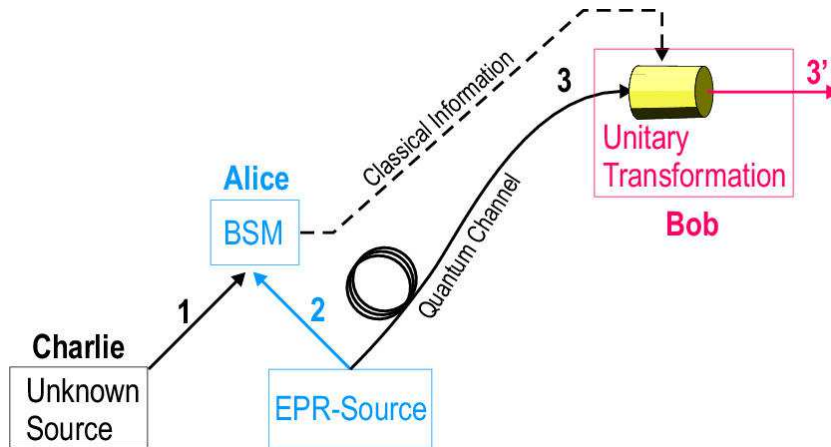


Fig. 28. Schematic of quantum teleportation of an unknown state. Particle 1 is given to Alice who subjects it to a Bell-state measurement (BSM) together with particle 2, the latter one being entangled to particle 3 (at Bob's). Depending on the result of this measurement, Bob applies a unitary transformation to particle 3 which then ends up in precisely the same state in which particle 1 was originally.

If, in some sense, the aim of quantum key distribution is the communication of classical bits, quantum teleportation, discovered in 1993 by Bennett *et al.*,¹³¹ can be thought of as being the exchange of quantum bits. One might define quantum teleportation as the art of transferring the state of an unknown qubit located at Alice's to a second quantum system, located at Bob's, the motivation being that it might be impossible to send the physical system itself. In this application of quantum communication, the qubit to be sent is unknown to the parties involved in the transfer, but it might be known to a third party, Charlie.

In a world of classical physics, teleportation is nothing remarkable. It suffices to measure the properties of the (classical) bit and then communicate the information about its composition to Bob, who then reconstructs the bit. This strategy must fail in the quantum case where the measurement of an unknown qubit without disturbing it is impossible and cloning is forbidden.^{132,133} Surprisingly, quantum communication provides a way out of this problem (see Fig. 28). Before Charlie hands over the particle to Alice who then teleports it to Bob, the latter have to share a pair of entangled particles. Alice now makes a Bell measurement on Charlie's particle and her part of the entangled pair (see Section 2.2.3). She thus projects the two-particle state randomly onto one of the four Bell states. Note that this measurement only reveals the joint state of both particles, but not the individual states. The outcome of this measurement projects Bob's particle onto one of four different states as well. Using two classical bits, Alice now tells Bob about the outcome of her measurement and depending on her message, Bob performs one of four

unitary operations on his particle: the identity operation, a bit flip, a phase flip, or a bit and a phase flip. This finally leaves it in the state of the particle Charlie had initially handed over to Alice, albeit neither Alice nor Bob know about this state. It is important to note that Charlie's particle is left in an arbitrary state after the Bell measurement, and that no cloning has taken place. Moreover, since Alice's classical information is needed to reconstruct the state of Charlie's particle, faster than light communication is not possible.

The experimental realization of quantum teleportation has invoked a strong reaction in the public. Whereas one can clearly say that quantum teleportation in its current form has no relation to disembodied transport of objects or even humans, it is also true that the idea to transmit a quantum state without sending a particle is an intriguing concept. Three different experiments based on polarization qubits have been reported.

- 1997 Bouwmeester *et al.*¹³⁴ are the first to demonstrate quantum teleportation based on a Bell measurement using linear optics. Although this allows in principle to teleport in 50% of all cases, only the projection onto the ψ^- state is used in the experiment. The result of the measurement is shown in Fig. 29.
- 1998 Boschi *et al.*¹³⁵ demonstrate a teleportation set-up in which all four Bell states can be identified — even using only linear optics. The entangled state is realized using k-vector (mode) entanglement, and the polarization degree of freedom of one of the entangled photons is employed to prepare the unknown state. However, this scheme can not be implemented for photons that come from independent sources as required for instance for entanglement swapping (see Section 4.4).
- 2001 Kim *et al.*⁵⁵ demonstrated quantum teleportation based on a Bell measurement implementing non-linear interaction. This enables a projection onto all four Bell states, however, with very small efficiency of around one out of 10^{10} . In order to compensate for the efficiency, the input state (send by Charlie) is a classical pulse from a fs laser. Nevertheless, this experiment shows that a complete Bell measurement is in principle possible, even when using single-photons and without having to take advantage of additional degrees of freedom of the entangled pair.

In addition, Furusawa *et al.*²⁰ demonstrated 1998 quantum teleportation based on continuous quantum variables.

4.4 Entanglement swapping

If we think of quantum teleportation as the transfer of an unknown (but still well defined) state we usually require that all states of the space we select are teleported perfectly. A natural extension is that any relation that the original particle has with respect to other systems should be transferred as well. Specifically, if our particle was entangled to another system we would require from a faithful teleportation machine that this entanglement is transferred to the particle that “inherits” the state at Bob's location.

This generalized concept, mentioned for the first time in 1993 by Żukowski *et al.*¹³⁶, has become known as entanglement swapping (or teleportation of entanglement). It sym-

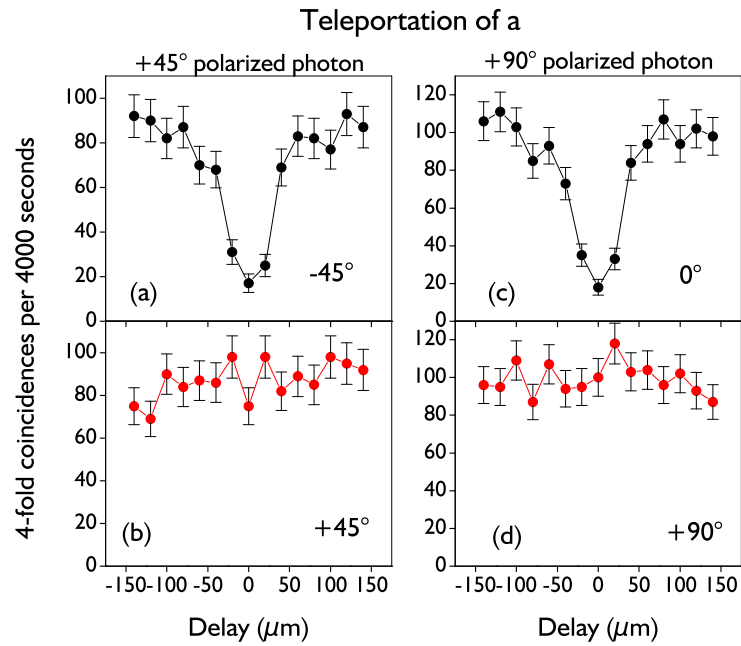


Fig. 29. Experimental data showing faithful teleportation of an independently created polarization qubit. Two linear polarization states are tested: 45° and 90° . The fidelity is roughly the same for both cases.

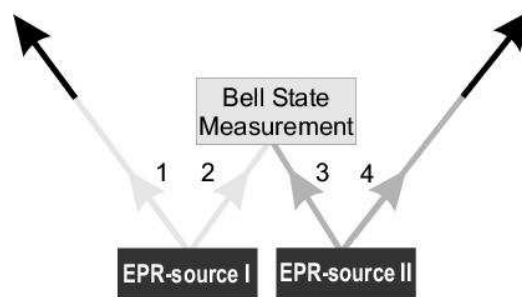


Fig. 30. Entanglement swapping between two EPR-pairs by a Bell-state measurement.

metrizes the teleportation scheme to a procedure that can be applied to two or more entangled systems.¹³⁷ The lowest order protocol joining two entangled two-qubit systems is depicted in Fig. 30. If, say, both entangled systems are produced in the $|\psi^-\rangle_{12}$ and $|\psi^-\rangle_{34}$ Bell-states, and we project onto a $|\psi^-\rangle_{23}$ state we find particles 1 and 4 in the state

$$\begin{aligned} \langle \psi^- |_{23} [|\psi^-\rangle_{12} \otimes |\psi^-\rangle_{34}] &= \\ &= \frac{1}{\sqrt{8}} [\langle 01 | - \langle 10 |]_{23} [|01\rangle - |10\rangle]_{12} \otimes [|01\rangle - |10\rangle]_{34} \\ &= \frac{1}{\sqrt{8}} [\langle 01 | - \langle 10 |]_{23} [|0101\rangle - |1001\rangle - |0110\rangle + |1010\rangle]_{1234} \\ &= \frac{1}{\sqrt{8}} [|01\rangle - |10\rangle]_{14} = |\psi^-\rangle_{14}. \end{aligned} \tag{16}$$

Therefore, particles 1 and 4 end up in an entangled state although they never interacted locally.

Any experimental verification of this protocol is a clear demonstration of the quantum physical projection postulate: the joint measurement of particles 2 and 3 results in a preparation of the joint state of particles 1 and 4, regardless of whether one decides to project on a product, or on an entangled state. In the specific case considered here, the projection postulate predicts the change of the joint state of particle 1 and 4 from a product state to an entangled state. This can easily be verified by subjecting particle 1 and 4 to a test of a Bell inequality.

A first attempt to demonstrate that the entanglement is indeed swapped has been reported by Pan *et al.*¹³⁸ in 1998. The experiment was based on polarization entanglement. However, although the observed degree of entanglement surpasses the limit of a classical wave theory, it was not high enough to manifest itself in a violation of a Bell inequality. Yet, after some refinements, Jennewein *et al.* could recently demonstrate a violation of Bell's inequality with "swapped" entanglement.¹³⁹ The measurements yielded $S^{\text{exp}} = 2.42 \pm 0.09$ which exceeds the limit of 2 for local realistic theories by 4 standard deviations.

4.5 Purification and distillation

In the context of extending quantum information protocols to larger distances, considerable interest has grown for measures against decoherence as encountered while transmitting quantum states through a noisy environment. Various schemes of entanglement distillation, purification and concentration, and of quantum error correction have been proposed (see references in ^{16,15}), however, to date, only one experimental demonstration of distillation of photonic entanglement has been reported.

As predicted by Gisin in 1996,¹⁴⁰ entanglement purification can be achieved by local filtering. This scheme has been demonstrated experimentally 2001 by Kwiat *et al.*⁵⁹ (Fig. 31). To demonstrate the phenomenon of "hidden non-locality", certain partially entangled, partially mixed states that do not violate Bell inequality were prepared utilizing the polarization entanglement source based on two stacked thin type-I crystals with their optic

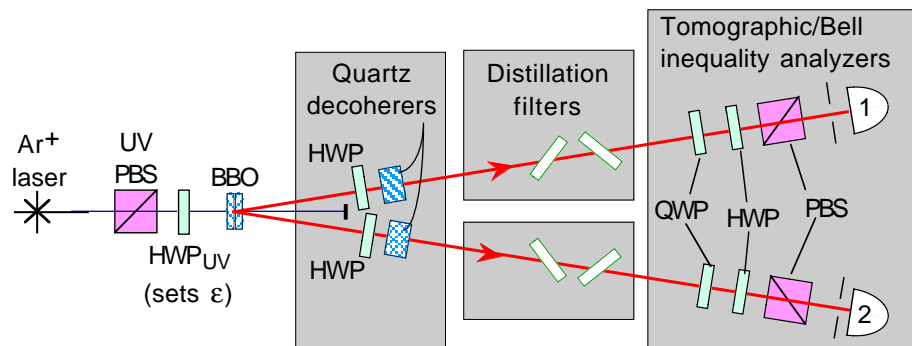


Fig. 31. Experimental setup to demonstrate entanglement distillation and hidden non-locality. Half-wave plates and two 1cm thick quartz elements (decoherers) allow to generate partially entangled, partially mixed states. After filtering they are analyzed by means of two qubit analyzers – either in order to reconstitute the density matrix via quantum tomography, or to test the CHSH Bell inequality.

axes at 90° as discussed in Section 2.2.2. It has been shown that the resulting states after a suitable local filtering operation violate Bell-CHSH inequalities (Fig. 32).

Actually, much more than from decoherence, applications of quantum communication like quantum cryptography suffer from transmission losses paired with detector noise.^q As argued in section 4.1, the fact that the QBER increases with losses (Eq. 15) limits the maximum transmission distance. A way out would be to use a quantum non-demolition (QND) measurement¹⁴¹ at Bob's and to switch on the detectors only if a photon is known to arrive (hence $\mu = 1$ and remaining $t_{\text{link}}=1$) (see Fig. 33). Unfortunately, QND measurements for detection of visible or telecommunication photons do not exist yet.^r Another possibility that is in reach with current technology is to use a concatenation of two-particle sources and Bell state measurements and to establish entangled photons at Alice's and Bob's via entanglement swapping. In this scheme, Bob's detectors are only switched on if Alice detected a photon *and* if the last Bell state measurement (at Bob's) was conclusive. It therefore much resembles a QND measurement. Interestingly, this idea is closely related to the original motivation for entanglement swapping:¹³⁶ testing Bell inequalities with "Event-Ready-Detectors". However, although this scheme allows to extend the maximum transmission span, it will at the same time significantly reduce the bit rate.

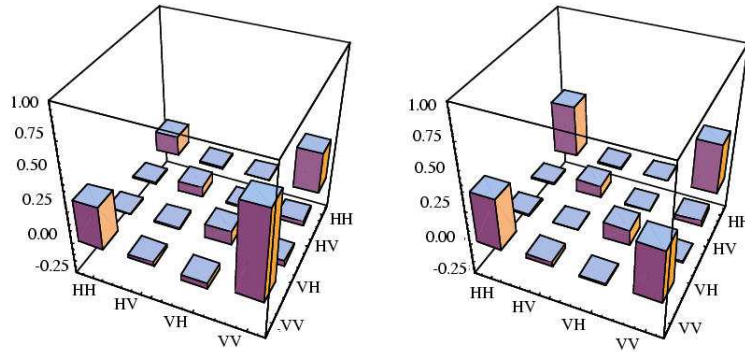


Fig. 32. Measured density matrices before (left) and after (right) distillation. A violation of CHSH Bell inequality is observed for the state after distillation ($S_{\text{filtered}}=2.22$) while the initial state does not manifest non-local behavior ($S_{\text{initial}}=1.82$)

^qThis contrasts with proposals for quantum computing using massive particles where the particles hardly get lost and good detectors exist, but where decoherence is the major problem.

^rQND measurements for microwave photons have recently been demonstrated by Nogues *et al.*¹⁴²

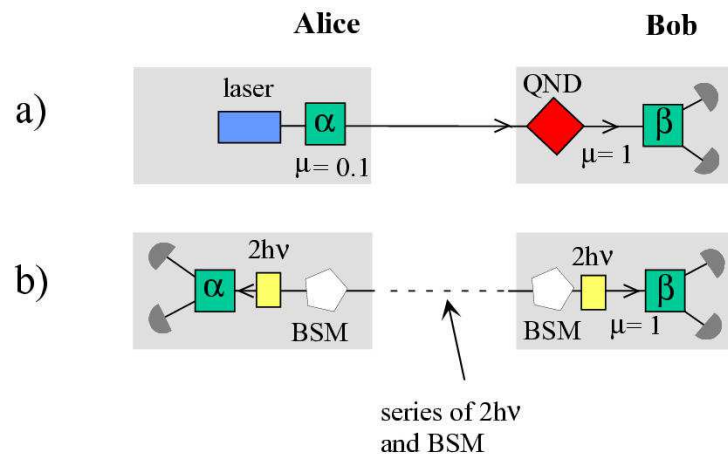


Fig. 33. Comparison of QND measurement based (a), and entanglement swapping based (b) realization of event ready detectors at Bob's. " $2h\nu$ " denote entangled two-photon sources, "BSM" a Bell-state measurement, and α and β are the settings at Alice's and Bob's qubit analyzers.

5 Conclusion

In this article, we tried to review the major developments in experiments based on entanglement of photonic qubits, both in the traditional domain of fundamental tests of quantum non-locality, as well as in the new approach of using entanglement as a resource for quantum communication. In traditional tests of spin 1/2 Bell-inequalities no major surprises are expected any more — at least concerning experiments with photons. But we are only at the very beginning of tests of non-locality using higher dimensional systems,¹⁴³ systems employing more than two particles (Section 3.2), or experiments testing other interpretations of the quantum world (Section 3.1.2). Furthermore, the fact that entanglement can be used as a resource for applications in quantum communication came like a great surprise and stimulated much interest in the physics as well as in the general community. Quantum cryptography is a good candidate of becoming the first industrial application, a development that would have a major impact on the whole field.

It is very interesting that tests of Bell-inequalities, traditionally considered part of fundamental research, recently became an application with the Ekert scheme for quantum cryptography, and are nowadays routinely employed in the laboratory to characterize the quality of the entanglement of photon pairs before passing on to more complicated experiments. However, not only the change from fundamental to applied aspects can be observed, the opposite is possible as well: It is for instance still an open fundamental question if the connection between security of quantum cryptography and violation of a Bell inequality can be generalized to all sorts of protocols.

The enormous progress obtained in laser and optical fiber technology, single photon detectors, and the availability of non-linear crystals enable nowadays experiments that were only gedankenexperiments not even long ago. However, new ideas and technology are needed for further steps. For instance, the secret bit rate and maximum transmission distance in quantum cryptography experiments are limited by the performance of detectors and single photon sources, and there is big need for efficient sources creating more than two entangled particles. Maybe photon sources based on individual nitrogen-vacancy color centers in diamond^{144,145}, quantum dots^{146,147,148} and parametric down-conversion in PPLN waveguides^{36,37} will turn out to enable more refined experiments in the future.

Although quantum non-locality has recently been observed with atoms, photons still play an outstanding role whenever it comes to experiments employing entanglement. They are best suited as a carrier of quantum information since decoherence effects due to interaction with the environment are very small. But unfortunately, photons do not interact with other photons, a major problem when it comes to Bell state measurements or processing of quantum information in general. A solution might be to map photonic quantum states onto massive particles like atoms or ions that are in principle well suited for all applications where two-particle interaction is needed. A first experiment in this context has been performed¹⁴⁹ very recently.

Acknowledgements

The authors acknowledge financial support by the Swiss FNRS and the Austrian Science Fund (FWF) project no. S1506, as well as by the IST-FET “QuComm” project of the European Commission, partly financed by the Swiss OFES. W. T. would like to thank his colleagues from GAP, especially N. Gisin and H. Zbinden for theoretical and practical support during the mentioned experiments. G. W. would like to thank T. Jennewein and A. Zeilinger for helpful discussions and continued support.

References

1. E. Schrödinger, *Naturwissenschaften* **23**, 807 (1935).
2. A. Einstein, B. Podolsky, and N. Rosen, *Phys. Rev.* **47**, 777 (1935).
3. J. Bell, *Physics* **1**, 195 (1964).
4. J. F. Clauser, M. A. Horne, A. Shimony, and R. A. Holt, *Phys. Rev. Lett.* **23**, 880 (1969).
5. J. F. Clauser and M. A. Horne, *Phys. Rev. D* **10**, 526 (1974).
6. S. J. Freedman and J. F. Clauser, *Phys. Rev. Lett.* **28**, 938 (1972).
7. A. Aspect, *Nature* **398**, 189 (1999).
8. P. Grangier, *Nature* **409**, 774 (2001).
9. W. H. Zurek, *Physics Today* **44**, 36 (1991).
10. G. C. Ghirardi, A. Rimini, and T. Weber, *Lett. Nouv. Cim.* **27**, 293 (1980).
11. A. Suarez and V. Scarani, *Phys. Lett. A* **232**, 9 (1997).
12. E. Hagley *et al.*, *Phys. Rev. Lett.* **79**, 1 (1997).
13. H. Zbinden, J. Brendel, N. Gisin, and W. Tittel, *Phys. Rev. A* **63**, 022111 (2001).
14. *Physics World* **11**, (1998).
15. *The Physics of Quantum Information*, edited by D. Bouwmeester, A. Ekert, and A. Zeilinger (Springer, Berlin, 2000).
16. H.-K. Lo, S. Popescu, and T. Spiller, *Introduction to quantum computation and information* (World Scientific, Singapore, 1998).
17. N. Gisin, G. Ribordy, W. Tittel, and H. Zbinden, *Rev. Mod. Phys.* (2001).
18. A. Zeilinger, *Sci. Am.* **282**, 50 (2000).
19. Z. Y. Ou, S. F. Pereira, H. J. Kimble, and K. C. Peng, *Phys. Rev. Lett.* **68**, 3663 (1992).
20. A. Furusawa *et al.*, *Science* **282**, 706 (1998).
21. C. Silberhorn *et al.*, *Phys. Rev. Lett.* **86**, 4267 (2001).
22. P. D. Townsend, *Opt. Fiber Tech.* **4**, 345 (1998).
23. R. Hughes, G. Morgan, and C. Peterson, *J. Mod. Opt.* **47**, 533 (2000).
24. H. Zbinden *et al.*, *Electron. Lett.* **33**, 586 (1997).
25. G. Ribordy *et al.*, *J. Mod. Opt.* **47**, 517 (2000).
26. S. N. Molotkov, *Journal of Experimental and Theoretical Physics* **87**, 288 (1998), quant-ph/9811038.
27. J.-M. Mérola, Y. Mazurenko, J.-P. Goedgebuuer, and W. Rhodes, *Phys. Rev. Lett.* **82**, 1656 (1999).
28. A. Mair, A. Vaziri, G. Weihs, and A. Zeilinger, *Nature* (2001), (in press).
29. H. Bechmann-Pasquinucci and W. Tittel, *Phys. Rev. A* **61**, 062308 (2000).
30. E. S. Fry and R. C. Thompson, *Phys. Rev. Lett.* **37**, 465 (1976).
31. A. Aspect, P. Grangier, and G. Roger, *Phys. Rev. Lett.* **47**, 460 (1981).
32. D. C. Burnham and D. L. Weinberg, *Phys. Rev. Lett.* **25**, 84 (1970).
33. Z. Y. Ou, C. K. Hong, and L. Mandel, *Phys. Lett. A* **122**, 11 (1987).
34. Z. Y. Ou and L. Mandel, *Phys. Rev. Lett.* **61**, 50 (1988).

35. C. K. Hong, Z. Y. Ou, and L. Mandel, *Phys. Rev. Lett.* **59**, 2044 (1987).
36. S. Tanzilli *et al.*, *Electronics Letters* **37**, 26 (2001), quant-ph/0012053.
37. K. Sanaka, K. Kawahara, and T. Kuga, *Phys. Rev. Lett.* **86**, 5620 (2001), quant-ph/0012028.
38. Y.-H. Kim *et al.*, *Phys. Rev. A* **63**, 062301 (2001).
39. T. Kiess, Y. Shih, A. Sergienko, and C. Alley, *Phys. Rev. Lett.* **71**, 3893 (1993).
40. P. G. Kwiat *et al.*, *Phys. Rev. Lett.* **75**, 4337 (1995).
41. P. G. Kwiat *et al.*, *Phys. Rev. A* **60**, R773 (1999), quant-ph/9810003.
42. J. G. Rarity and P. R. Tapster, *Phys. Rev. A* **41**, 5139 (1990).
43. P. H. S. Ribeiro, quant-ph/0009112 (unpublished).
44. J. Brendel, N. Gisin, W. Tittel, and H. Zbinden, *Phys. Rev. Lett.* **82**, 2594 (1999).
45. T. Keller, M. Rubin, and Y. Shih, *Phys. Lett. A* **244**, 507 (1998).
46. Y.-H. Kim, M. Chekhova, S. Kulik, and Y. Shih, *Phys. Rev. A* **54**, R37 (1999).
47. J. D. Franson, *Phys. Rev. Lett.* **62**, 2205 (1989).
48. J. Brendel, E. Mohler, and W. Martienssen, *Europhys. Lett.* **20**, 575 (1992).
49. P. G. Kwiat, A. M. Steinberg, and R. Y. Chiao, *Phys. Rev. A* **47**, 2472 (1993).
50. M. Michler, K. Mattle, H. Weinfurter, and A. Zeilinger, *Phys. Rev. A* **53**, R1209 (1996).
51. K. Mattle, H. Weinfurter, P. G. Kwiat, and A. Zeilinger, *Phys. Rev. Lett.* **76**, 4656 (1996).
52. N. Lütkenhaus, J. Calsamiglia, and K.-A. Suominen, *Phys. Rev. A* **59**, 3295 (1999).
53. J. Calsamiglia and N. Lutkenhaus, *Appl. Phys. B* **72**, 67 (2001).
54. P. G. Kwiat and H. Weinfurter, *Phys. Rev. A* **58**, R2623 (1998).
55. Y.-H. Kim, S. P. Kulik, and Y. Shih, *Phys. Rev. Lett.* **86**, 1370 (2001).
56. M. Żukowski, A. Zeilinger, and H. Weinfurter, *Annals of the N.Y. Acad. of Sciences* **755**, 91 (1995).
57. A. G. White, D. F. V. James, P. H. Eberhard, and P. G. Kwiat, *Phys. Rev. Lett.* **83**, 3103 (1999).
58. J. Řeháček, Z. Hradil, and M. Ježek, *Phys. Rev. A* **63**, 040303(R)1 (2001).
59. P. G. Kwiat, S. Barazza-Lopes, A. Stefanov, and N. Gisin, *Nature* **409**, 1014 (2001).
60. D. M. Greenberger, M. Horne, and A. Zeilinger, in *Bell's Theorem, Quantum Theory, and Conceptions of the Universe*, edited by M. Kafatos (Kluwer Academic, Dordrecht, The Netherlands, 1989), pp. 69–72.
61. M. Żukowski, A. Zeilinger, M. Horne, and H. Weinfurter, *Acta Phys. Pol. A* **93**, 187 (1998).
62. M. Hillery, V. Bužek, and A. Berthiaume, *Phys. Rev. A* **59**, 1829 (1999).
63. A. Rauschenbeutel *et al.*, *Science* **288**, 2024 (2000).
64. C. A. Sackett *et al.*, *Nature* **404**, 256 (2000).
65. J.-W. Pan and A. Zeilinger, *Phys. Rev. A* **57**, 2208 (1998).
66. W. Tittel, H. Zbinden, and N. Gisin, *Phys. Rev. A* **63**, 042301 (2001).
67. D. Bohm, *Phys. Rev.* **85**, 166 (1952).
68. D. Bohm, *Phys. Rev.* **85**, 180 (1952).
69. J. S. Bell, *Speakable and Unsayable in Quantum Mechanics* (Cambridge UP, Cambridge, 1987).
70. D. Bohm, *Phys. Rev.* **108**, 1070 (1957).
71. S. Kochen and E. Specker, *J. Math. Mech.* **17**, 59 (1967).
72. J. S. Bell, *Rev. Mod. Phys.* **38**, 447 (1966).
73. C. Simon, M. Żukowski, H. Weinfurter, and A. Zeilinger, *Phys. Rev. Lett.* **85**, 1783 (2000).
74. J. F. Clauser, *Phys. Rev. Lett.* **36**, 1223 (1976).
75. W. Perrie, A. J. Duncan, H. J. Beyer, and H. Kleinpoppen, *Phys. Rev. Lett.* **54**, 1790 (1985).
76. T. Pittman, Y. Shih, A. Sergienko, and M. Rubin, *Phys. Rev. A* **51**, 3495 (1995).
77. P. Kwiat *et al.*, *Phys. Rev. A* **60**, R773 (1999).
78. P. Tapster, J. Rarity, and P. Owens, *Phys. Rev. Lett.* **73**, 1923 (1994).
79. D. Strelakov *et al.*, *Phys. Rev. A* **54**, R1 (1996).

80. A. A. et al., Phys. Lett. B **422**, 339 (1998).
81. A. Aspect, P. Grangier, and G. Roger, Phys. Rev. Lett. **49**, 91 (1982).
82. A. Aspect, J. Dalibard, and G. Roger, Phys. Rev. Lett. **49**, 1804 (1982).
83. Y. H. Shih and C. O. Alley, Phys. Rev. Lett. **61**, 2921 (1988).
84. J. G. Rarity and P. R. Tapster, Phys. Rev. Lett. **64**, 2495 (1990).
85. W. Tittel *et al.*, Phys. Rev. A **57**, 3229 (1998).
86. W. Tittel, J. Brendel, H. Zbinden, and N. Gisin, Phys. Rev. Lett. **81**, 3563 (1998).
87. G. Weihs *et al.*, Phys. Rev. Lett. **81**, 5039 (1998).
88. M. A. Rowe *et al.*, Nature **409**, 791 (2001).
89. W. Tittel, J. Brendel, H. Zbinden, and N. Gisin, Phys. Rev. Lett. **84**, 4737 (2000).
90. D. Mermin, Physics Today **38**, 38 (1985).
91. C. Kurtsiefer, M. Oberparleiter, and H. Weinfurter, quant-ph/0101074 (unpublished).
92. P. Pearle, Phys. Rev. D **2**, 1418 (1970).
93. E. Santos, Phys. Lett. A **212**, 10 (1996).
94. N. Gisin and B. Gisin, Phys. Lett. A **260**, 323 (1999).
95. P. H. Eberhard, Phys. Rev. A **47**, R747 (1993).
96. W. H. Furry, Phys. Rev. **49**, 393 (1936).
97. W. Tittel, J. Brendel, N. Gisin, and H. Zbinden, Phys. Rev. A **59**, 4150 (1999).
98. E. Santos, Phys. Lett. A **200**, 1 (1995).
99. J. S. Bell, Journal de Physique **42**, C2 41 (1981).
100. N. Gisin and H. Zbinden, Phys. Lett. A **264**, 103 (1999).
101. G. Ghirardi, A. Rimini, and T. Weber, Phys. Rev. D **34**, 470 (1986).
102. D. Bohm, *Quantum Theory* (Prentice-Hall, Englewood Cliffs, 1951).
103. L. Hardy, Phys. Rev. Lett. **68**, 2981 (1992).
104. V. Scarani, W. Tittel, H. Zbinden, and N. Gisin, Phys. Lett. A **276**, 1 (2000).
105. P. Eberhard, private communication (unpublished).
106. D. Bouwmeester *et al.*, Phys. Rev. Lett. **82**, 1345 (1999).
107. J.-W. Pan *et al.*, Nature **403**, 515 (2000).
108. N. D. Mermin, Physics Today **43**, 9 (1990).
109. J.-W. Pan *et al.*, Phys. Rev. Lett. **86**, 4435 (2001).
110. C. A. Fuchs *et al.*, Phys. Rev. A **56**, 1163 (1997).
111. D. Mayers, Journal of the Association of Computer Machinery, (in press) quant-ph/9802025.
112. C. H. Bennett *et al.*, J. Cryptology **5**, 3 (1992).
113. S. Wiesner, Sigact news **15**, 78 (1983).
114. C. H. Bennett and G. Brassard, in *Proceedings of the International Conference on Computer Systems and Signal Processing* (PUBLISHER, Bangalore, India, 1984), pp. 175–179.
115. C. H. Bennett, Phys. Rev. Lett. **68**, 3121 (1992).
116. G. Ribordy *et al.*, Electron. Lett. **34**, 2116 (1998).
117. N. Lütkenhaus, Phys. Rev. A **61**, 052304 (2000).
118. G. Brassard, N. Lütkenhaus, T. Mor, and B. C. Sanders, Phys. Rev. Lett. **85**, 1330 (2000).
119. C. K. Hong and L. Mandel, Phys. Rev. Lett. **56**, 58 (1986).
120. A. K. Ekert, Phys. Rev. Lett. **67**, 661 (1991).
121. C. Bennett, G. Brassard, and N. D. Mermin, Phys. Rev. Lett. **68**, 557 (1992).
122. A. Ekert, J. G. Rarity, P. R. Tapster, and G. M. Palma, Phys. Rev. Lett. **69**, 1293 (1992).
123. N. Gisin and B. Huttner, Phys. Lett. A **228**, 13 (1997).
124. V. Scarani and N. Gisin, quant-ph/0104016 (unpublished).
125. T. Jennewein *et al.*, Phys. Rev. Lett. **84**, 4729 (2000).
126. D. S. Naik *et al.*, Phys. Rev. Lett. **84**, 4732 (2000).
127. D. Enzer, P. Hadley, G. Peterson, and P. G. Kwiat, private communication (unpublished).
128. D. Bruss, Phys. Rev. Lett. **81**, 3018 (1998).

129. H. Bechmann-Pasquinucci and N. Gisin, *Phys. Rev. A* **59**, 4238 (1999).
130. G. Ribordy *et al.*, *Phys. Rev. A* **63**, 012309 (2001).
131. C. H. Bennett *et al.*, *Phys. Rev. Lett.* **70**, 1895 (1993).
132. W. Wootters and W. Zurek, *Nature* **299**, 802 (1982).
133. D. Dieks, *Phys. Lett. A* **92**, 271 (1982).
134. D. Bouwmeester *et al.*, *Nature* **390**, 575 (1997).
135. D. Boschi *et al.*, *Phys. Rev. Lett.* **80**, 1121 (1998).
136. M. Żukowski, A. Zeilinger, M. A. Horne, and A. K. Ekert, *Phys. Rev. Lett.* **71**, 4287 (1993).
137. S. Bose, V. Vedral, and P. L. Knight, *Phys. Rev. A* **57**, 822 (1998).
138. J.-W. Pan, D. Bouwmeester, H. Weinfurter, and A. Zeilinger, *Phys. Rev. Lett.* **80**, 3891 (1998).
139. T. Jennewein, J.-W. Pan, G. Weihs, and A. Zeilinger, to be published (unpublished).
140. N. Gisin, *Phys. Lett. A* **210**, 151 (1996).
141. P. Grangier, J. A. Levenson, and J.-P. Poizat, *Nature* **396**, 537 (1998).
142. G. Noguez *et al.*, *Nature* **400**, 239 (1999).
143. J. C. Howell, A. Lamas-Linares, and D. Bouwmeester, quant-ph/0105132 (unpublished).
144. C. Kurtsiefer, S. Mayer, P. Zarda, and H. Weinfurter, *Phys. Rev. Lett.* **85**, 290 (2000).
145. R. Brouri, A. Beveratos, J.-P. Poizat, and P. Grangier, *Opt. Lett.* **25**, 1294 (2000).
146. J.-M. Gérard *et al.*, *Phys. Rev. Lett.* **81**, 1110 (1998).
147. J. Kim, O. Benson, H. Kan, and Y. Yamamoto, *Nature* **397**, 500 (1999).
148. A. Kiraz *et al.*, *Appl. Phys. Lett.* **78**, 3932 (2001).
149. B. Julsgaard, A. Kozhekin, and E. Polzik, quant-ph/0106057 (unpublished).